SAI/1999-060/Rp

POST-OPERATIONS CROSS-CALIBRATION STATUS REPORT

v1.0

June 7, 1999

P. García-Lario

1 Introduction

1.1 Scope

This document summarises the current status of cross-calibration activities at the ISO Data Centre (IDC) as of June 8, 1999. It includes updated information on the latest achievements in the calibration of all four ISO instruments with special emphasis on cross-calibration aspects as well as an assessment of progress according to the POPS Cross-calibration Plan presented at the last NDC's Coordination Meeting.

Part of it also constitutes the natural extension of the series of reports issued by Calibration Liaison during the Operational Phase and now falling within the framework of POPS activities.

This Status Report is the first of a series of reports that will be generated by the IDC every 6 months culminating in the final POPS Cross-calibration Status Report at the end of the Post-Operations phase.

1.2 Structure of cross-calibration activities

The global IDC strategy for approaching cross-calibration during the Post-Operations phase, as previously described in the ISO POPS Cross-calibration Plan, is based on topic-oriented Working Groups, each one of them addressing one specific calibration topic.

Working Groups are formed by members from the IDC and from the different NDCs. They are also open to contributions from external individuals interested in actively participating in ISO calibration activities.

Currently, seven Working Groups (WG, hereafter) have been created and are actively working on:

- Aperture/Beam Profiles, PSFs and Straylight
- Glitch Effects
- Line profiles
- Photometric calibration
- Polarisation
- Spectral Matching and RSRF
- Transients

Of course, these areas overlap in many cases and many cuts through the calibration issue are possible. For example, studies of *Transients* are fundamental to a full understanding of the instruments' photometric calibration, which is the main goal of the *Photometric Calibration* WG. The WG scheme provides them with a platform to exchange their knowledge and to progress with respect to their own subject.

It is the responsibility of cross-calibration to maintain an overview of the work of the several Working Groups, cooperate with instrument-specific calibration manpower in efforts to understand inconsistencies of calibration relevant to more than one instrument and establish links between the different Working Groups when necessary favouring a fluid exchange of useful information.

An overview of the composition of each of these WGs can be found at:

`http://www.iso.vilspa.esa.es/users/expl_lib/ISO/WG_COMPOSITION.PS`

1.3 Final Goals: General

The objectives of cross-calibration can be summarized as follows:

- Compare the results of different ISO instruments and verify the errors quoted for each instrument-specific calibration. Where these results appear to be inconsistent seek to understand and to eliminate those differences.

- Compare ISO results with external data (e.g. ground based observations, KAO data, IRAS, COBE, ...). Where results appear to be inconsistent seek to understand and to eliminate those differences.

- Verify that, from a more global point of view, the calibrations of the individual ISO instruments are correct, and ensure a certain level of homogeneity and consistency of the data and how they were calibrated (e.g. compatibility of models, bandpass zero-points, and of calibration philosophy and procedures).

The intention is to have a flexible plan/strategy with these goals as a reference and to materialize this in a detailed schedule of cross-calibration activities for each of the Working Groups listed above.

Responsibility for cross-calibration planning is with the IDC in close interaction with the NDCs which are responsible for instrument-specific calibration.

1.4 Final Goals: per Working Group

1.4.1 Aperture/Beam Profiles, PSFs and Straylight

· Characterization of the instruments' beam profiles.

· Address common problems (asymmetries, vignetting, ghosts,..) and their possible relation to the ISO telescope PSF.

· Allow cross-fertilisation of models available (e.g. ASAP software).

· Evaluation of common deconvolution tools, to apply to extended source data, once beam profile calibration files become available.

· Support improvement of ISO pointing reconstruction in OLP.

1.4.2 Glitch Effects

· Statistical analysisis and characterization of glitches in the four ISO instruments. Study of the relation with the space radiation environment.

· Compare glitch statistics and glitch height distributions with model predictions and simulations.

· Enhance the quality of the reduced ISO data, improving the de-glitching and de-tailing algorithms in the pipeline and/or IA.

· Keep the knowledge on the radiation environment and its effects on the detectors, so that it can be applied to future missions, in particular FIRST.

1.4.3 Line profiles

· Characterize the SWS and LWS observed instrumental profiles.

· Study the stability of these instrumental profiles as a function of time, forward and backward scans, detector, line strength and point-like versus extended sources.

· Analysis and interpretation of deviations found from line profile definition; recommendations and caveats.

· Comparison with theoretical instrumental profiles and resolution.

1.4.4 Photometric calibration

· Definition of the photometric system and description of calibration sources/models used in ISO data reduction.

· Characterization of the photometric accuracies achieved for each ISO AOT (photometric 'error budget').

· Make periodic 4-instrument photometric comparisons on selected sample targets and extend this comparison to calibration models and to photometric results obtained with other facilities (DIRBE/IRAS/KAO, ground-based,..) using OLP data products.

· Make similar comparisons on a subsample of targets using data reduced with the latest available versions of the instrument IAs and compare this with OLP photometric accuracies.

· Testing of photometric improvements as new algorithms or calibration files as they become available stimulating their inclusion into the corresponding IAs first and eventually into the pipeline.

- Identification and analysis of photometric calibration problems affecting OLP data products providing recommendations and caveats to the users of the ISO Legacy Archive.

1.4.5 Polarisation

- Characterization of the polarimetric capabilities of ISO. Angles, detection limits, wavelength dependency, internal consistency (PHT,CAM) and comparison with external data.

1.4.6 Spectral Matching and RSRF

- Characterization of the Relative Spectral Response Function (RSRF) for all ISO spectroscopic observations.
- Analysis of spectral matching between LWS and SWS in the overlapping region. Same with CAM-CVF and PHT-S spectra. Comparison with models.
- Identification of possible systematic errors in the measured spectral response to extended sources by comparing the observations from a variety of instruments. Effects on the determination of spectral line fluxes.
- Expansion of cross-calibration between the instruments beyond the wavelength regions which they have in common.

1.4.7 Transients

- Characterize transient effects in the 4 ISO instruments and determine the best correction method as a function of detector type, observing mode and characteristics of the source and estimation of effects on photometric accuracy.
- Develop S/W tools to detect and correct transient effects in IA first and eventually implement these tools in OLP if possible.

1.5 Meetings

The dates of the latest meetings, all of them held at VILSPA, are listed below per WG in alphabetical order together with the dates when the next meetings have provisionally been scheduled.

Working Group	Last meeting	Next meeting
Beam profiles:	April 23, 1999	July 30, 1999
Glitches:	January 27, 1999	September 17, 1999
Line profiles:	April 27, 1999	September 1999
Photometric calibration:	February 23, 1999	September 1999
Polarisation:	May 28, 1999	September 1999
Transients:	April 30, 1999	September 1999
Spectral Matching and RSRF:	May 7, 1999	September 1999

2 Review of Cross-calibration Plan

2.1 Overview of Working Group activities

As it was defined in the ISO POPS Cross-calibration Plan, the WGs should:

- look at major calibration issues across instrument boundaries
- identify problems, (interim-)goals and milestones (usually linked to OLP milestones)
- trigger/recommend further work, and recognise imperatives in their area
- establish and pursue relevant contacts in NDCs
- identify good calibration sources and strategies.

In order to achieve these goals each WG was requested to define a list of actions, goals and milestones with an associated schedule which was used as initial basis for the Cross-calibration Plan. This plan will be reviewed every 6 months in a series of Status Reports of which this is the first issue.

2.1.1 List of actions closed

A number of actions originally included in the Cross-calibration Plan can now be considered closed. In the following, a summary of the main results found and conclusions reached is provided sorted by WG. In some cases, comments on milestones not directly related with activities carried out by members of a WG are included when they are relevant for the future planning of the WG or to illustrate a progress on the current understanding of a problem under analysis by that specific WG. For instance, the celebration of a Workshop on extended sources at VILSPA, like the one scheduled next September at VILSPA, is not an activity of the *Beam Profile* WG but certainly will have an impact on the activities of this WG. Another example could be the implementation of a new transient correction tool in CIA which, although not effectively carried out by any of the members of the *Transients* WG, is here considered an important milestone for the WG.

Beam Profiles :

```
BP: Description of the  telescope PSF  to be used as input for the
     beam profile models of the  various  instruments. First draft
     in  "ISO  telescope  PSF model"  by Koryo Okumura  (February
     1999).
```

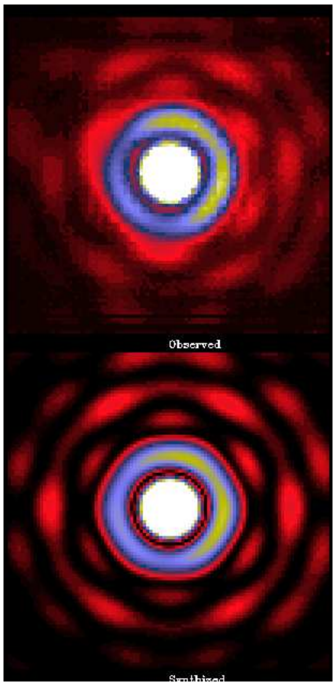

Figure 1: Observed (top) and synthesized (bottom) PSFs: 1.5 arcsec PFOV at LW9 - Koryo Okumura

In the last meeting of the Beam Profiles WG Koryo Okumura reported on the latest results obtained using ASAP software simulations with coherent light. It seems that a lateral displacement in the secondary mirror of ISO of 0.3 mm can explain the assymetric PSF observed (see Figure 1). A revision of the *ISO telescope PSF model* document by Koryo Okumura is expected by September 1999.

- The latest status reports on beam profiles per instrument were also presented at the last WG meeting:

- For CAM a library of PSF's is already available and the characterization of ghost reflections is on-going by Koryo Okumura (status will be reviewed at the next WG meeting in September 1999).

- PHT expects to have updated beam profile calibration files for PHT-S and PHT-C for the next OLP version 8.4 in August 1999. The fraction of PSF falling on each C200 pixel has been determined for a number of typical pointing configurations, using calibration observations (asteroids, outer planets and the bright star HR 5340). Comparisons between the measured values and model expectations show strong discrepancies for some of the C200 filters. The empirical values can be used to improve the C200 point source photometry in minimaps, source-background pointings, and to decide whether a given source is extended. The full report by Rene Laureijs can be found at

  `http://www.iso.vilspa.esa.es/users/expl_lib/PHT/c200fpsf02.ps.gz`

- LWS is making an analysis of the instrument beam profile using observations of Mars with some difficulties in the interpretation of the beam observed which seems narrower than expected and also assymetric with fringing and unstitching affecting the outer parts of the beam (see Figure 2). For the time being only the core of the LWS 'mean beam' has been characterised by Chris Lloyd. Conversion factors from point source to extended source flux calibration (Jy $\rightarrow$ Jy/sr) will be determined from the mean beam and included in ISAP 2.0 (release expected by July 1999).

- Finally, for SWS the combination into one file of all SWS beam profile measurements has been completed by Rosario Lorente. Douwe Beintema is now working towards an updated version of the optical model, fine tuned to fit the measurements, which is expected to be available at the next WG meeting in September 1999.

- Concerning ISO pointing reconstruction, Andy Pollock reported that the S/W now considers guide star aberration and proper motion (making use of Tycho data). Tests are still on-going and implementation in the pipeline is expected in OLPv8.6 version (November 1999).

- A major milestone in the activities of this WG will be the organization by the Community Support Group of the IDC at VILSPA of a Workshop on *ISO beyond point sources: studies of extended infrared emission* on 14-17 September 1999. The latest information on this Workshop can be found at:

`http://www.iso.vilspa.esa.es/meetings/isobeyond/`

- The WG encourages usage of the ISO PSF model developed by Okumura as input for the beam profile models of the other instruments and the study of

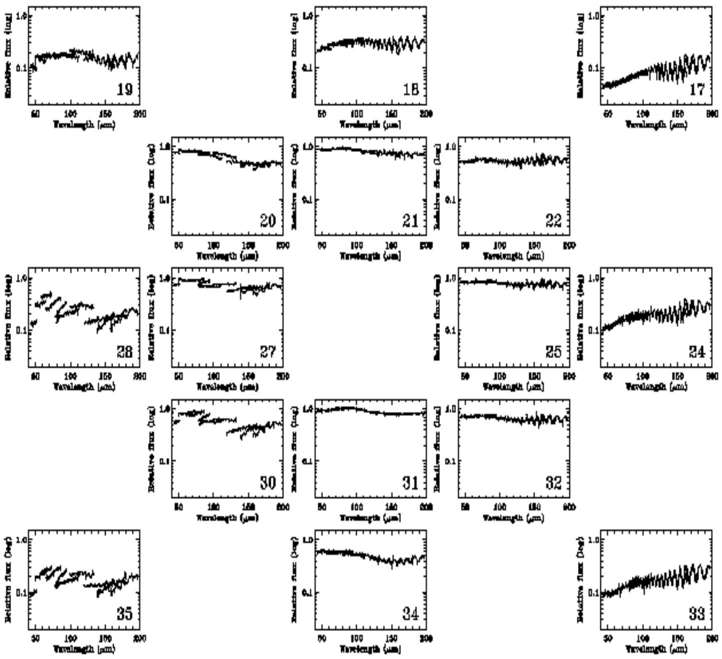

Figure 2: Relative fluxes for the inner region of the LWS beam obtained on Mars. In this plot P.A. 30 is vertical - Chris Lloyd

possible application of deconvolution tools and simulations in general to other instruments.

<u>Glitches:</u>

```
GL: Analysis of glitch statistics and glitch height distributions
     in the four ISO instruments available in  "The ISO detectors
     and the space  radiation environment"  by  Ana Heras  et al.
     (November 1998);  final results  and  comparison with models
     expected by April 1999.
```

- The document above cited, presented at the ESA Workshop on Space Weather (11-13 November 1998, ESTEC) is available at

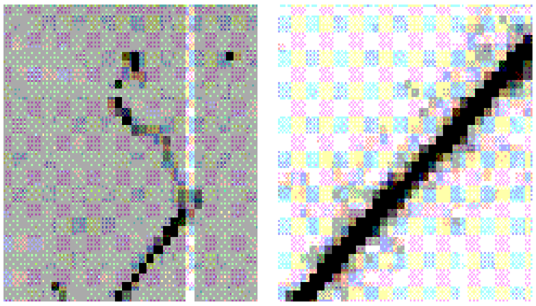

Figure 3: Examples of particle impacts on ISOCAM. On the left panel a low energy particle impact has probably stopped in the detector, while on the right panel a heavy ion passin through can be seen - Ana Heras et al.

`ftp://astro.estec.esa.nl/pub/aheras/iso_gwg/spweather.ps`

According to the results presented in this document the glitch rates differences found between instruments are probably related to the efficiency of the algorithms used in detecting the smaller glitches. However, the glitch height distribution for LWS is puzzling, since the contribution from the high energy impacts is much lower than in the other instruments and also compared with model predictions. Apart from a special shielding, no other explanation is found. Petteri Nieminen is performing simulations of the radiation effects on the LWS detectors which include the production of secondaries and delta-rays in the instrument shield (to be completed by August 1999).

The possible effect of particle impacts leading to saturation in SWS in the glitch counting and how this would affect glitch statistics has also been investigated. The results obtained indicate that saturation plays a minor role since the percentage of saturating glitches not counted in the SWS glitch rates is estimated to be ~3% in the Si:Ga band 2 and ~9% for the Ge:Be band 4.

GL: Predictions on the glitch rate and glitch height distribution expected in solar minimum and solar maximum conditions in the FIRST/PACS detectors (April 1999).

- Helmut Feuchtgruber presented at the last Glitches WG meeting the results of a simulation of radiation effects on the PACS detectors. Based on the glitch rates and glitch height distribution observed in SWS detectors and taking into account the characteristics of the PACS electronics and detectors, it is possible to predict how the output signal of PACS would be affected by glitches (tails not considered). He concludes that most of them can be detected at the ramp

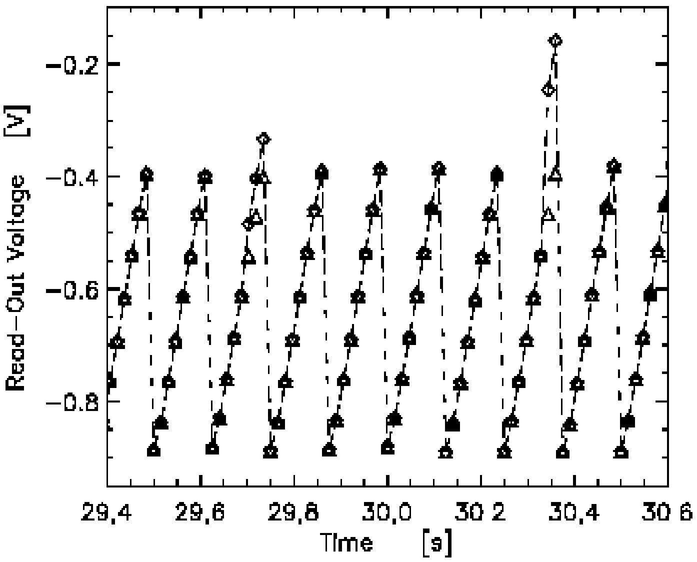

Figure 4: Details of a deglitched measurement, showing affected ramos, before (diamonds) and after deglitching (triangles) with the simple ERD correction - Carlos Gabriel/Jose Acosta

level and that most of the glitches can be removed through sigma clipping and the original S/N reconstructed.

In collaboration with Petteri Nieminen, he has also calculated the glitch rates expected during solar maximum and minimum in the PACS detectors. The conclusion is that $\sim$ 20 days per year of overwhelming proton fluxes are expected during solar maximum, in which probably no PACS observations will be possible.

`GL: Study of the possible inclusion of a more sophisticated PIA deglitching algorithm in PHT pipeline (April 1999).`

- Currently available deglitching algorithms in ISOPHOT pipeline are based on simple statistical analysis. They basically search for deviating values within a distribution of differences between two consecutive read-outs (see Figure 4) or, on a higher level, between signals (see Figure 5) removing the data affected. Glitches affect mostly detectors based on Ge:Ga (P3, C100 and C200), whereas those based on Si are less affected (P1, P2 and PHT-S). Unfortunately, transients and hysteresis effects make the detection of glitches sometimes not easy. Satisfactory results are usually obtained by the application of a simple correction at ERD level followed by a second one at SPD level.

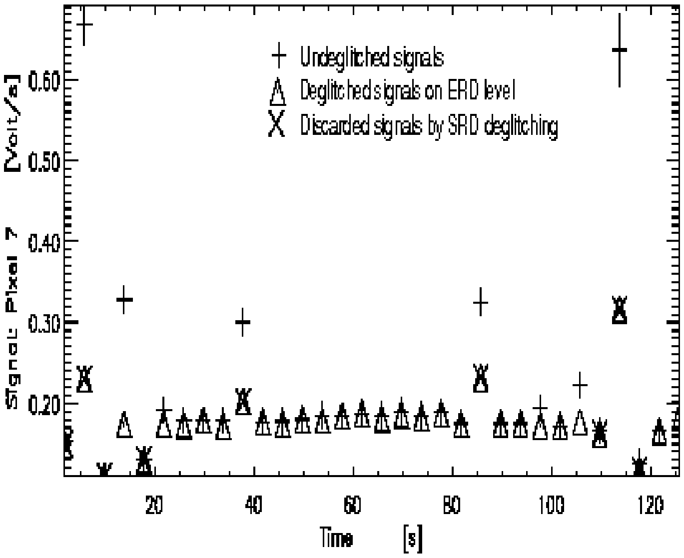

Figure 5: Comparison of signals from the same measurement, processed with (triangles) and without (plus symbols) read-out de-glitching procedure. Although most of the data disturbances produced by glitches are corrected at the ramp (ERD) level, residual effects are still present, which are recognized and flagged (crossed) by the signal de-glitching procedure - Carlos Gabriel/Jose Acosta

However, there are two ways of deglitching data at the ERD level: the simple approach, currently implemented in the pipeline, discards deviating signals above a certain threshold. A more sophisticated approach which identifies the glitch and also looks for a possible subsequent tail discarding deviating signals above a second threshold would be desirable. The results of the investigations carried out indicate that the simple approach works very well on intermediate brightness sources but cannot be applied to very bright sources for which ramps contain only a few read-outs. The sophisticated approach considers several ramps at once and, thus, can be used to de-glitch measurements with only a few read-outs per ramp which cannot be handled by the first method (the case of bright sources). In addition, it also consider two thresholds in order to reject tails following primary glitches and this is well suited for observations of low flux sources when glitches produce long tails which otherwise are not detected.

The implementation of this more sophisticated de-glitching method in the pipeline at ERD level has been postponed to OLP version 9 (May 2000) since it requires a different approach to the problem (the correction is applied at read-out level and not at ramp level).

- An overview on the effect of glitches on PHT data and a more detailed description of the different correction methods currently implemented in PIA is contained in *Deglitching methods by the ISOPHOT Interactive Analysis (PIA)* by Carlos Gabriel and J.A. Acosta-Pulido available at:

`http://www.iso.vilspa.esa.es/manuals/PHT/pia/public/det_ws_98.ps`

- The latest progress reports on de-glitching/de-tailing CAM, LWS and SWS data can be found in the minutes of the last WG meeting at

`ftp://astro.estec.esa.nl/pub/aheras/iso_gwg/minutes_2.pdf`

ISOCAM glitches have been characterized by Arnaud Claret (3 types are identified) in *ISOCAM Glitch Library* by Arnaud Claret and Hervé Dzitko available at

`http://www.iso.vilspa.esa.es/users/expl_lib/CAM/glitch_lib/`

and de-glitching algorithms are discussed in *Glitch effects in ISOCAM LW detector* by Claret et al. (Experimental Astronomy, 1999). Improved de-glitching methods have already been implemented in CIA by Stephan Ott.

De-glitching correction algorithms (automatic and interactive) are also available under SWS IA. Work on the discrepant LWS glitch height distribution found is on-going.

- From the experience obtained from the analysis of glitches in ISO data the WG recommends to the FIRST project the inclusion of the Standard Radiation Environment Monitor (SREM) or a similar instrument in order to have independent measurements of the radiation environment which will be crucial for the understanding of the radiation effects on the PACS instrumentation.

Line profiles:

`LP: Preliminary analysis of LWS line profile stability with time, scan direction, detector and wavelength for three lines in NGC6543 presented in the last LDAG meeting (October 1998).`

- The analysis carried out by Rosario Lorente and Cecile Gry on three lines (52, 57 and 88 μm) in NGC 6543 shows a strong stability of the LWS line profile (with deviations always below the 4% level for a given line/detector combination). In general, the profiles found are always very similar with the exception of the 57 μm line detected on SW2 which presents an extended wing in the blue side not yet understood (see Figure 6). Therefore, average SW profiles

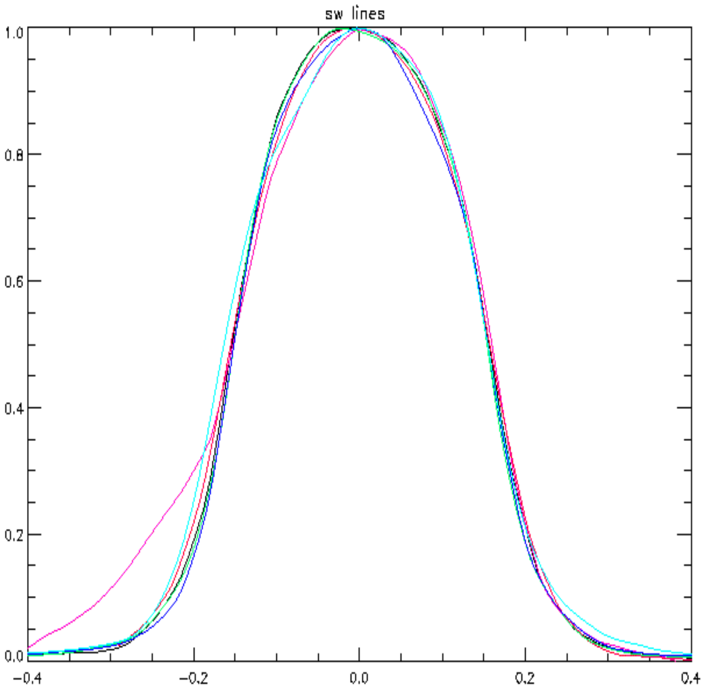

Figure 6: LWS line profiles observed in NGC 6543, NGC7027 and NGC 6826. The plot includes the mean profiles observed at 52 μm (as observed on the SW2 and SW3 detectors), 57 μm (on SW2 and SW3), 63 μm (on SW3) and 88 μm (on SW5). The only discrepant assymetric profile corresponds to the 57 μm line detected on the SW2 detector - Rosario Lorente

have been computed for each SW line/detector pair excluding the 57 μm line on SW2.

- Recently the analysis has been extended to other lines in NGC 6543 and to two other objects: NGC 7027 and NGC 6826. The results obtained confirm the stability of the LWS line profiles and the problems affecting the line at 57 μm in the SW2 detector. Investigations on possible reasons for the assymetry observed in this line are on-going. In particular, the possible connection with an unidentified emission detected on the blue side of the 57 μm line on some Fabry-Pérot spectra is being investigated.

- Anna di Giorgio has looked at the grating line profiles predicted by ray-tracing performed in LAS before launch for a few wavelengths. The comparison with the computed grating profiles is very good at the top of the line although it fails to reproduce the wings, which are wider than predicted.

- Emmanuel Caux presented at the last WG Meeting the first results of his analysis of the Fabry-Pérot emission line profiles observed in NGC 7023 and NGC 7027 at 63, 145 and 158 μm. The resulting profiles are very similar to the expected ones except for the assymetries observed on the right edge of these lines which are possibly due to memory effects. These have first to be understood before a definite profile can be produced. (see new actions under the *Transients WG* subsection).

```
LP: Determination of the  SWS spectral resolution and instrumental
     line profile as  measured by the full resolution modes  SWS02
     and SWS06. Preliminary results in "ISO-SWS grating resolution
     and  instrumental profile as measured by the  full resolution
     modes SWS02 and SWS06" by Dieter Lutz et al. (April 1999).
```

- This document is still in the form of an advance draft (MPE-ISO-99-1) and includes the analysis of assymetries and deviations from gaussian shape found and the effects of mispointing and transients on line profiles making use of measurements on several sources of different types. The profiles are found to be wavelength-dependent and detector-dependent. This work will be completed by September 1999. The goal is to create a database to be used by SWS calibration experts to evaluate the instrumental profile and to provide the resulting information to the users together with possible tools within OSIA.

- The SWS01 line profile study was already completed in September 1998 and described by Rosario Lorente in the document *Spectral resolution of SWS AOT 1*.

In this study, FWHMs and spectral resolutions are derived from gaussian fittings to line profiles observed in NGC 6543 and NGC 7027 as a function of scanning mode and wavelength.

Photometric calibration:

```
PH: Development  of  Atlas tool  for  cross-calibration  purposes
     between SWS and LWS by Ekkehard Wieprecht and Alberto Salama
     (May 1999). Applicable to PHT and CAM data soon (June 1999).
```

- Atlas is an IDL-based tool which allows direct comparison of SWS and LWS ISO survey products. From an input list of TDTs created with an SQL query to the ISO Data Archive, it provides with $m \times n$ plots on single pages for easy comparisons of a number of targets (see Figure 7). Some IDL post-processing is also carried out like flux units conversion and automatic scaling for pairs of SWS-LWS spectra on the same target.

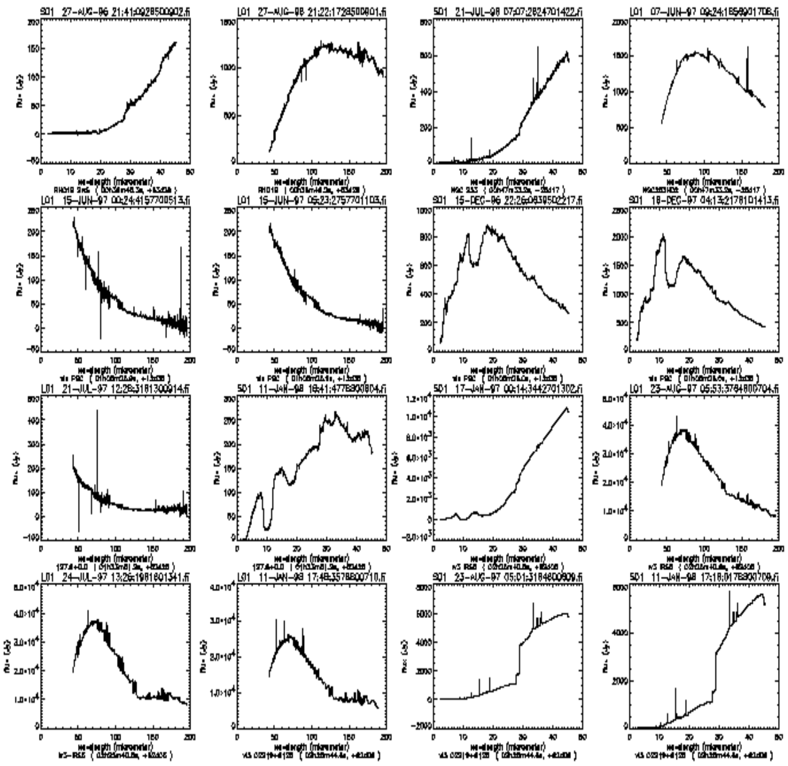

Figure 7: An example of the $m \times n$ plots that can be obtained with the Atlas tool - Alberto Salama

Further development (applicability to PHT and CAM survey products) is on-hold awaiting the results of a comparative study of tools currently available or expected to be available in the near future (see below the new action on Spectral Matching WG) which will recommend the use - and additional development if needed - of only that one considered to be more adequate and powerful for cross-calibration purposes. This is intented to avoid duplication of functionalities and unnecessary workload on single-tool developers.

The latest progress reports on absolute flux calibration of individual instruments were presented at the last meeting of the Photometric Calibration WG on February 23, 1999:

- **CAM:**

  The main uncertainty in the photometry of CAM is the fact that signals do not reach a stable value by the end of the measurement. Especially for low fluxes this can lead to large errors. Several transient correction methods exist in CIA to correct for this. The latest implemented method is the so-called Fouks-Schubert method, which is claimed to reach accuracies on the percent level. The method is however best suited for extended emission and fails for structures with strong spatial gradients (like point sources). More details are given under the *Transients WG* subsection below. Evaluation results (presented later in this document) confirm this significant improvement.

  The latest report on CAM accuracy is contained in the *ISOCAM Calibration Accuracies Document* by Joris Blommaert and Diego Cesarsky (November 1998) available at:

  `http://www.iso.vilspa.esa.es/manuals/CAM/accuracies/cam_accur/`

- **SWS:**

  The latest status report on SWS photometry was presented by Pat Morris at the SWS consortium meeting on January 25, 1999. The following partial results were reported:

  - Investigation of the uncertainties connected to memory effects shows a segregation into low, moderate and high flux regimes.

  - Stability of the flux scale derived in a calibration revolution was estimated to be: Band 1: 1%; Band 2: 19%; Band 3: 9%; and Band 4: 25%.

  - Investigation of the beam profile is on going. This will allow to improve flux determination for less well centred measurements and extended objects (see *Beam Profile WG* subsection).

  - From OLPv8.4 onwards, uncertainties in flux calibration of data products will be specified and made up from three parts: standard deviation (from the fitting of the ramps themselves), offset (from dark current correction) and gain.

  - Uncertainties of the dark correction can lead to large errors (10%) at the edges of the spectrum.

  - An *End-of-Mission Report on SWS Flux Calibration* by Pat Morris is in preparation.

  - A document describing the current *SWS Calibration Status* as of March 1999 is available at:

  `http://www.iso.vilspa.esa.es/users/expl_lib/SWS/SWS_Cal_Accuracy.html`

- **LWS:**

  - The RSRF in the LWS-calibration files has been derived with the wrong model of Uranus. It will be replaced in next OLP delivery with a slightly modified RSRF which improves the match between model and observations of Mars (see more details below under the *Spectral Matching WG* subsection).

  - A document describing the current *LWS Calibration Status* as of November 1998 is available at:

  `http://www.iso.vilspa.esa.es/users/expl_lib/LWS/LWS_Cal_Accuracy.html`

- **PHT:**

  - Concerning Signal non-linearity Bernhard Schulz reports examples of calibration measurements on celestial standards which demonstrate that the detector has a non-linear response. Data used to calibrate the internal radiation sources (FCS) with celestial standards became more consistent after linearisation. Implementation of the signal linearisation correction in the data processing is planned to be introduced in OLPv8.4 (August 1999). Since it is applied early in the signal processing chain, it requires the redetermination of several Cal-G files. Considerable changes of photometric results are however only expected in cases where the signals of the sky measurement and the FCS measurement are very different like in multi-filter AOTs.

  - Concerning calibration of PHT chopped measurements, a new calibration method developed at MPIA was presented by Bernhard Schulz. The new technique promises better robustness against glitches and a better correction for the signal losses. It makes use of the periodicity of the measurements and constructs a characteristic pattern, representing both signal levels - on source and off source - by 8 data points. Three classes of patterns were already distinguished: a linear case, a curved case and an overshooting case. Presently MPIA is busy determining the relations between these patterns and the associated staring observations of source and background. Also this new step is expected to be part of OLPv8.4.

  - The latest report concerning PHT calibration status is contained in the document *ISOPHOT Calibration Accuracies* by Ulrich Klaas et al. (October 1998) available at:

  `http://www.iso.vilspa.esa.es/manuals/PHT/accuracies/pht_accuracies20/`

- Note that one of the main tasks of the *Photometric Calibration WG* consists in the evaluation of calibration improvements reported every six months in the Calibration Status Report affecting OLP and/or IA data products and the investigation of the possible discrepancies found between models and observed fluxes or between instruments. This work will be done on set of targets (stars, cloud, galaxies, ...) which will be selected on the basis of the specific problem under analysis. The results obtained will then be reported in the next Cross-calibration Status Report with an assessment on the progress achieved and/or the problems found and recommendations on possible new calibration aspects to explore in order to improve the quality of ISO data.

Polarisation:

- Progress is currently being focused on the characterisation of the polarimetric capabilities of ISO. Determination of polarisation angles, detection limits, wavelength dependency, internal consistency (PHT,CAM) and comparison with external data.

The latest reports on polarisation data have been presented at the *Workshop on ISO Polarisation Observations*, organized by the Community Support Group of the IDC at VILSPA on May 25-28, 1999. The contributions presented at this meeting will be posted at

`http://www.iso.vilspa.esa.es/meetings/polarisation/`

- **PHT:**

  - New polarisation routines written by Ulrich Klaas have been implemented in PIA.

  - The fractional polarisation is consistent in each instrument. However, there is at present a debate on the polarisation angle for PHT. Inconsistencies found among the C200 pixels from field to field suggest that the background used might be in some cases significantly polarised. A report will be presented at the next WG meeting (September 1999). Consequently PHT polarisation data are not yet ready for publication. It is felt that the basic issues (leading to more consistency) should be solved first by the instrument experts.

- **CAM:**

  - Analysis of CAM polarisation measurements on point sources by Ralf Siebenmorgen is on-going. The problem here is the still imperfect transient and de-glitching algorithms available and the time consuming interactive process of the data analysis. Apart from this, the quality of the results obtained is good and well correlated polarisation vectors/degrees are found.

Spectral Matching and RSRF:

```
SM: Spectral matching analysis of all targets in the ISO Archive
     with  2-200 micron spectroscopy available using Atlas tool.
     Selection of the sample (May 1999)
```

- With the help of the Atlas tool Alberto Salama selected a a flux limited ($>$ 100 Jy at 44 μm) sample of targets from the ISO Data Archive observed with both LWS01 and SWS01 AOTs for cross-calibration comparison. The sample is composed of a total of 153 SWS01 and 242 LWS01 spectra corresponding to 122 astronomical sources (note that in some cases the same source was observed several times). The goal is to evaluate the degree of matching between SWS and LWS in the overlapping region in order to investigate the origin of previously reported matching problems affecting specific targets. Premilinary results are presented later in this document but investigations are still on-going. A report is expected by July 1999 (see list of new actions below).

- Discontinuities between SW1 and SW2 bands in LWS need also to be investigated since the correct absolute flux level in SW1 is essential for a meaningful comparison between LWS and SWS. This will also be analized with the help of the Atlas tool (see again list of new actions below).

- In addition, the possible effect of transients in band 4 (Ge:Be) of SWS have also been investigated by Fred Lahuis. Transient effects in SWS band 4 are different for forward and backward scans because there are dark current measurements after each down-scan (unlike LWS, where they are performed only at the beginning and the end of the observation). The conclusion found is that they amount only to less than 10% in band 4 of SWS and should have a negligible effect on SW1 band of LWS. Thus, they are probably not the reason for the discontinuities observed between LWS and SWS.

```
SM: Spectral  matching  analysis of  sample sources  observed  with
     CAM-CVF, PHT-S and SWS using new PHT calibration method (April
     1999).
```

- The results obtained with the new dynamic calibration method applied to PHT-S measurements of the asteroid Hygiea presented by Thomas Müller significantly improve the agreement between PHT-S and SWS data up to a few percent level (see a detailed description of these results under *Section 4* in this document).

- Latest report currently available on SWS RSRF by Bart Vandenbussche (February 1997) is contained in *RSRF calibration and implications* can be found at

`http://www.iso.vilspa.esa.es/users/expl_lib/SWS/rsrf`

The *End-of-Mission SWS RSRF* document by Bart Vandenbussche is still in preparation.

- The effects of instrumental fringing in the long wavelength section of the SWS (from 12 μm to 29μm) is a result of Fabry-Pérot effects within the instrument. Direct application of the SWS RSRF to the data quite often gives unsatisfactory results. The fringe residuals are significantly large and this limits the detection and analysis of weak spectral features. The fringes as they appear in the data are sometimes shifted with respect to the fringes in the RSRF when the source is not exactly at the centre of the aperture or if the source is extended. Also the width of the features can change depending on the extent of the source.

A number of methods have been developed within OSIA to adapt, change or correct these effects. They can reduce the residuals down to a level of 1−2%. A list of techniques that can be applied to the data with examples can be found in *ISO-SWS Data Analysis* by Fred Lahuis and Ekkehard Wieprecht (March 1999) available at:

`http://www.iso.vilspa.esa.es/users/expl_lib/SWS/lahuisf.ps.gz`

- The LWS RSRF derived with the wrong model of Uranus will be replaced by a slightly modified RSRF in the next OLP delivery (August 1999). Both are based on models provided by Griffin & Orton. With the new RSRF a better agreement is found between model and observations of Mars (see Figures 8 and 9). The re-calculated Neptune spectrum turns down at short wavelengths.

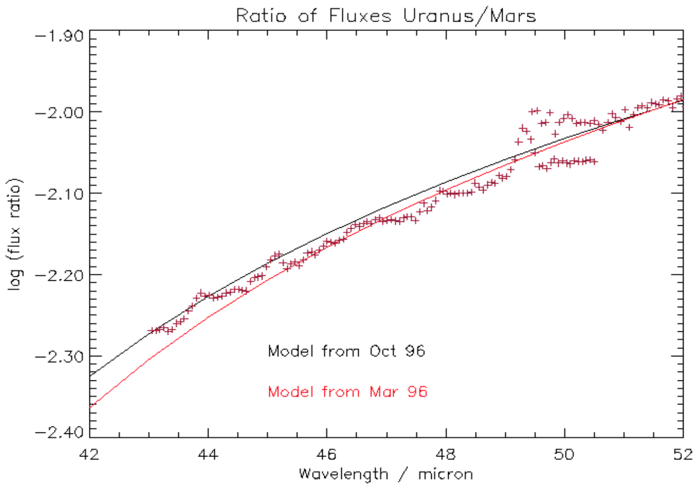

Figure 8: Observed Uranus/Mars flux ratios compared with predictions, in the 42−52μm spectral range, using the old (red) and the new (black) Uranus model - Martin Burgdorf

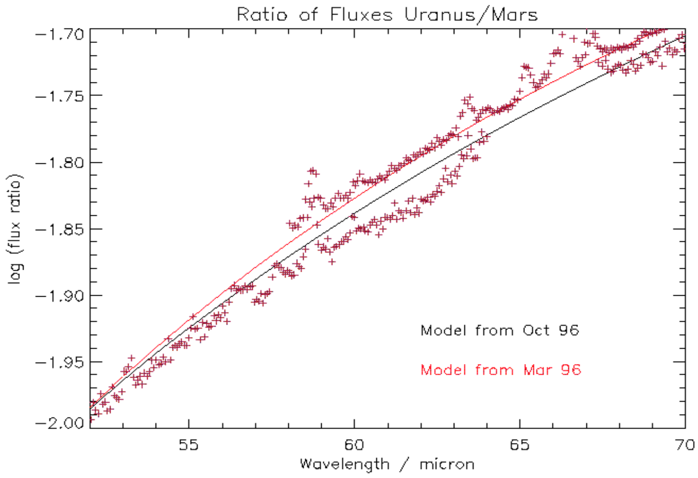

Figure 9: Observed Uranus/Mars flux ratios compared with predictions in the 52−70μm spectral range, using the old (red) and the new (black) Uranus model - Martin Burgdorf

An overview of different models for the calibration sources Uranus and Neptune was given by Martin Burgdorf in the last Spectral Matching WG Meeting on May 7, 1999. All models used for this comparison (by Lellouch, Abbas and Griffin & Orton) were derived using Voyager data and are still uncertain concerning the H_2/He mixing ratio and P/T profiles. Lellouch's model includes methane in his model. The differences in the fluxes predicted are typically smaller than 15%.

- A comparison of the LWS spectra from Mars and Uranus made by Bruce Swinyard with the final aim of investigating whether Mars can be used as discriminator between the different models used for Uranus and, at a later stage, Neptune confirmed the latest model by Griffin & Orton within the measured uncertainties of about 10%. The reason for this relatively big error is the very high flux of Mars, which makes necessary the use of low bias measurements to avoid non-linearities. The problem is that Uranus at low bias is too faint to obtain a very high S/N ratio. It was agreed at the last Spectral Matching WG to try to check the flux calibration in the overlapping region of the two spectrometers also with Callisto as standard. Since a black-body model for Callisto is probably a too simple approximation, a model for the moon of Jupiter is needed. This is a new action item on this WG and it is listed below as such.

- Finally, Helmut Feuchtgruber presented a report at the last WG Meeting on non-linearities in the SWS detectors, discussing in particular the example of Mars. A correction factor as a function of λ is found which removes the effect of debiasing. The spectrum of Mars, however, is also affected by partial (pre)saturation and imperfect RC time constants; all of this has to be dealt with for all pixels of band 4 before a sensible comparison with LWS and the available models can be performed. A summary of dominating sources for non-linearities in SWS Ge:Be readouts is also presented in this report as a function of the incident signal in the detector where it is shown that for low flux levels the dominant source of non-linearity is the so-called *reset pulse after-effect* while imperfect RC constants, debiasing and saturation effects become important only with increasing incident fluxes.

Transients:

`TR: Implementation of several transient correction methods in PIA: IAS empirical model for P3, C100 and C200 detectors (Ge:Ga); Fouks-Schubert model for P1 and P2 filters (Si-based) and chopped PHT-S measurements; and dynamic calibration method for PHT-S staring observations selected as best choices (March 1999).`

- Transients correction under PIA now include several possibilities depending on the AOT/technique used:

· Drift recognition: based on the identification of the stabilized part of a measurement (implemented in PIA and OLP since 1996).

· Fouks-Schubert model fitting: applicable to chopped PHT-S measurements and PHT-P1 and -P2 filters (implemented in PIA since 1998).

· Empirical IAS solution: applicable to the far infrared detectors P3, C100 and C200 based on exponential fits to data (implemented in PIA since 1998).

· Dynamic calibration: based on comparisons to temporal behaviour of calibration observations. Valid for PHT-S staring observations (implemented in PIA since February 1999 - PIA v7.3). 10% accuracy level achieved.

· Repetitive signal pattern solution: applicable to PHT-S chopped measurements (internally implemented in PIA - expected to be generally available from v7.4). Consistency checks with CAM data made by N. Lu indicate a 20% level of agreement.

`TR: Fouks-Schubert model and IAS inversion method implemented in CIA. Evaluation of different methods (April 1999).`

- A new IAS method to correct for transients based on an analytical inversion of the Fouks-Schubert model (see technical notes of Abergel and Coulais on the CAM instrument page at

`http://www.iso.vilspa.esa.es/users/expl_lib/CAM_list.html)`

has recently been implemented in CIA. For LW ISOCAM data, application of the new IAS correction method improves significantly the accuracy of the measurements.

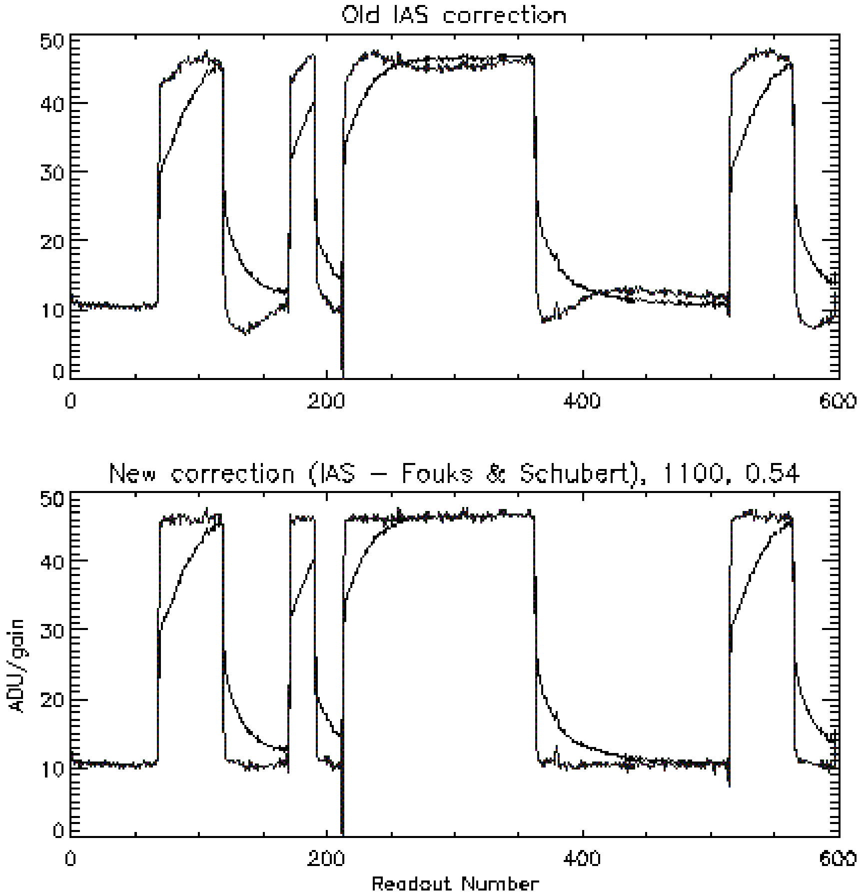

Figure 10: Comparison of inversions with the old IAS method (top) and with the new method (bottom). The mean value of the central square is plotted as a function of the readout number - Alain Coulais

Data analysis originally affected by a 30% photometric uncertainty improves up to a 10-15% level with the old IAS method and can be better than 1% with the new IAS method (see Figure 10). On the other hand, evaluation of Fouks-Schubert's transients correction method works better (accuracies on the percent level) for analysis of extended emission but fails for structures with strong spatial gradients (like point sources). Nevertheless, the method does improve the photometry when looking at the integrated value of the pixels under the PSF.

`TR: Analysis of transient effects on band 2 (Si:Ga) and band 4 (Ge:Be) and possible trends with signal/gain. Application of Fouks-Schubert model to SWS data. Comparison of SWS band 4 behaviour with LWS SW1 band (April 1999).`

- An empirical description of transients as they are observed in the SWS products has been carried out by Fred Lahuis. The intention is to get a large database in an attempt to parameterise the transients observed and thus help in the development of correction models. This is being done by Do Kester, who has succesfully adapted the Fouks-Schubert model for the correction of transients in SWS band 2 detectors. Transient effects are shown to be evident at the start (long wavelength ends) of the scans. They are particularly noticeable in bands 2A and 2C. With the adapted Fouks-Schubert model (only for band 2 so far) the transients are corrected to a high degree (see Figures 11 and 12). The corrections work well in not extremely bright sources (where other effects are present) decreasing the noise by a factor of 5 in some cases.

Investigations on the effect of transients on band 4 SWS data and their connection with the discontinuities observed in the SWS/LWS overlapping region are on-going. The preliminary conclusion is that they cannot account for the mismatches observed (at least not alone) between SWS and LWS (see previous reference to this work under the *Spectral Matching WG* subsection above).

- The latest progress reports per instrument were presented at the last Transients WG Meeting on April 30, 1999. The situation for PHT and CAM is in what can be considered an advanced stage. Several transients correction algorithms are currently implemented in PIA and CIA and they are relatively well understood in their applicability as a function of the AOT/detector used.

- Efforts will be concentrated in the near future on the extension of the transients correction in CAM data to point sources (see list of new actions below) and the understanding of transients in SWS and LWS. Soon transients correction tools based on the Fouks-Schubert method will be available under OSIA.

- Concerning LWS, Florence Vivares reported on results obtained on the analysis of transients in LWS parallel mode data. An *ad-hoc* correction has been applied which fit transients and tests if corrected data look better than

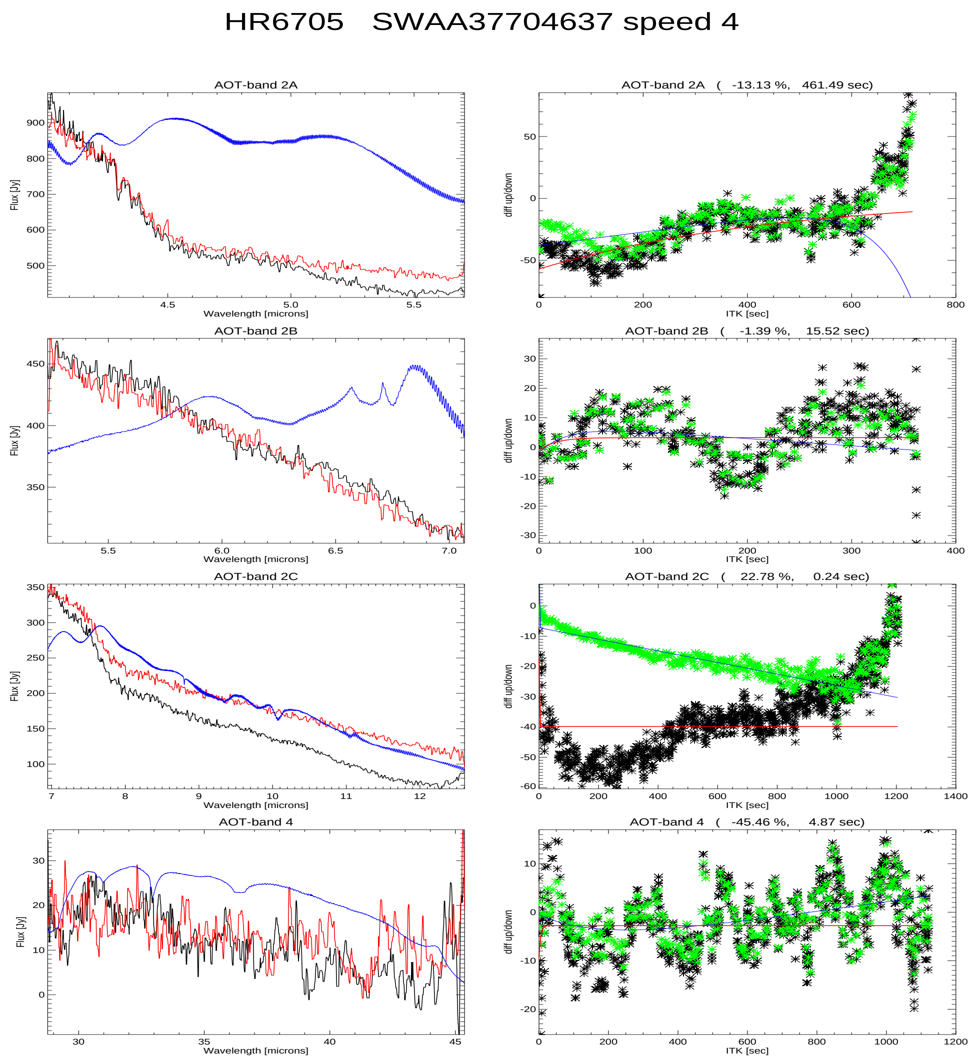

Figure 11: Standard OLP pipeline product corresponding to an observation of γ Draconis. Black shows the up scan and red the down scan. The transient effects are evident at the start (long wavelength ends) of the scans. They are particularly noticeable in bands 2A and 2C. In the right panels, the differences between the up and the down scans are plotted. The red and blue lines are exponential fits to the differences in respectively the AAR and SPD. This gives an impression of the magnitude of the transient effect - Fred Lahuis

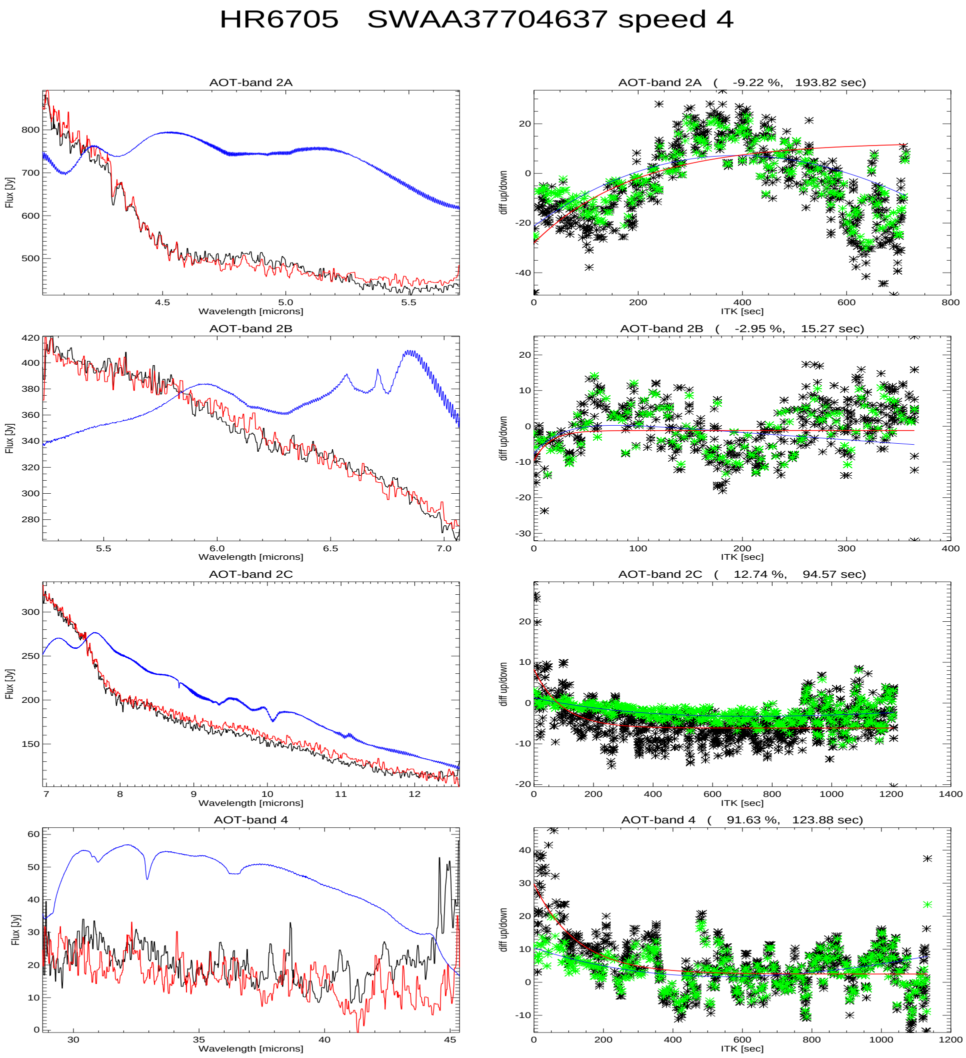

Figure 12: Same as Figure 11, but this time for the observation corrected with the adapted Fouks-Schubert method (only for band 2). The transients are corrected to a high degree. Residual offsets remain but it is likely that other non-transient effects (e.g. a dependency of the dark-current with temperature) play a role here - Fred Lahuis

the original. It is basically a numerical fit based on a combination of exponential functions and associated time constants, not a physical model. Efforts are concentrated on bands LW1 (where a good fit is found with only one time constant) and LW2 to LW4 (where two time constants are used). For bands SW1 to SW4, memory effects are often lost in their intrisic noise (mainly SW1 for which de-tailing correction is missing). The effects on SW5 and LW5 are too faint to be corrected. Emmanuel Caux found evidences of memory effects on some Fabry-Perot line profiles under study (see list of new actions below).

2.1.2 List of new actions

Some new actions have been defined since the last issue of the Cross-calibration plan. They are listed below sorted per WG.

Beam Profiles:

```
BP: ISO telescope assymetric PSF model document updated (September 1999)
Koryo Okumura
BP: New ISO Pointing reconstruction Cal-G files containing Tycho data
     for guide stars implemented in OLP (November 1999)
Andy Pollock
BP: Application of new ISO pointing reconstruction to SWS data on
     gamma-Dra in order to determine whether observed flux changes
     can be attributed to mispointing (August 1999)
Alberto Salama + Helmut Feuchtgruber
```

Photometric calibration:

```
PH: Definition of selected sample of targets (stars, clouds,
     galaxies, ...)  on  the  basis of  specific calibration
     problems under  analysis for cross-calibration purposes
     (September 1999)
Pedro Garcia-Lario
PH: Evaluation  of calibration improvements recently achieved
     and investigation on cross-calibration problems reported
     in the last Status  Report affecting OLP and/or  IA data
     products (every six months)
```

Polarisation:

```
PO: Analysis of the PHT polarisation inconsistencies found
      among the C200 pixels (September 1999)
Rene Laureijs
```

Spectral Matching and RSRF:

```
SM: Comparative study of cross-calibration tools: Atlas/IDA/UDF/PIA
     (July 1999)
Alberto Salama/Pedro Garc\'\i a-Lario
SM: Investigation on  SWS/LWS mismatches.  Identify possible role of
     extended and variable emission to explain the discrepant values
     found (July 1999)
Pedro Garcia-Lario
SM: Investigation on discontinuities found between SW1 and SW2 bands
     in LWS and possible trends with source properties (July 1999)
Alberto Salama
SM: Definition of a thermophysical model for Callisto (July 1999)
Thomas Mueller
```

Transients:

```
TR: Application of Fouks-Schubert transient correction method to
    point sources in ISOCAM data (September 1999)
Alain Coulais
TR: Characterization of memory effects affecting Fabry-Perot LWS
    line profiles  (September 1999)
Emmanuel Caux
TR: Implementation in public PIA version 7.4 of calibration of PHT-s
     chopped measurements. Transients correction method applicable to
     PHT-s chopped observations based on repetitive signal pattern (PHT)
Carlos Gabriel
TR: Transients correction tool based on the Fouks-Schubert method for
     SWS data available under OSIA (September 1999)
Fred Lahuis + Do Kester
```

2.2 Updated overall schedule

Below is the updated schedule for cross-calibration activities in the framework of the important events (impacting instrument calibration) during POPS. It contains all on-going actions previously identified and reported in the Cross-calibration Plan which are still pending as well as the new actions listed in the previous subsection. It is an objective of the next release of the ISO POPS Cross-calibration Plan to include an improved diagramme representation of this schedule.

```
==============================================================================
        * First Post-ops X-Cal. Status Report            08 Jun. 1999
            (OLPv7 and IAs cross-calibration)
==============================================================================

BP: SWS Beam profile model (June 1999)
Douwe Beintema
BP: SWS Beam profile calibration files (July 1999)
Rosario Lorente + Alberto Salama
BP: SWS Pointing Correction Tool (July 1999)
Rosario Lorente + Alberto Salama
GL: Implementation of  second-order de-tailing in LWS IA and pipeline,
     flagging data affected by glitches (June 1999)
BP: Characterization of the LWS Beam profile: conversion factors from
     point source to extended source fluxes available in ISAP 2.0
     (July 1999)
Chris Lloyd
SM: Comparative study of cross-calibration tools: Atlas/IDA/UDF/PIA
     (July 1999)
Alberto Salama/Pedro Garc\'\i a-Lario
SM: Investigation on  SWS/LWS mismatches.  Identify possible role of
     extended and variable emission to explain the discrepant values
     found (July 1999)
Pedro Garcia-Lario
SM: Investigation on discontinuities found between SW1 and SW2 bands
     in LWS and possible trends with source properties (July 1999)
Alberto Salama
SM: Definition of a thermophysical model for Callisto (July 1999)
Thomas Mueller
GL: Implementation of Do Kester's de-glitching method in SWS IA (August
     1999)
Do Kester
BP: PHT C100,C200 beam profile calibration files ready and implemented
     in OLP (August 1999)
Rene Laureijs
BP: Application of new ISO pointing reconstruction to SWS data on
    gamma-Dra in order to determine whether observed flux changes
    can be attributed to mispointing (August 1999)
Alberto Salama + Helmut Feuchtgruber
PHT: Non-linearity corrections in PHT data implemented in OLP (August
      1999)
PHT: New MPIA calibration method for chopped measurements implemented
      in PHT OLP (August 1999)
```

```
===============================================================================
         * OLP 8.4 (SWS+PHT) IDC --> NDCs                    04 Aug. 1999
===============================================================================
         * Deliveries for OLPv8.6 (major LWS upgrade)       13 Aug. 1999
===============================================================================


GL: Advanced  modelling  of  radiation  impacts (including production of
     secondaries) and effect of shielding on the observed glitch rates.
     Application of shielding studies to PACS detectors (August 1999)
Petteri Nieminen
BP: Workshop:  "ISO Beyond point sources: studies of extended infrared
     emission" to be held at VILSPA (September 1999)
BP: ISO telescope assymetric PSF model revision (September 1999)
Koryo Okumura
LP: Determination of the SWS spectral resolution and instrumental line
     profile as measured by the full resolution modes  SWS02 and SWS06.
     Final results (September 1999)
Dieter Lutz
PH: Definition of selected sample of targets (stars, clouds,
     galaxies, ...)  on  the  basis of  specific calibration
     problems under  analysis for cross-calibration purposes
     (September 1999).
Pedro Garcia-Lario
SM: Analysis of spectral line fluxes; comparison with external
    - KAO - data (September 1999)
Martin Burgdorf
PO: Analysis of the PHT polarisation inconsistencies among the C200
     pixels (September 1999)
Rene Laureijs
TR: Application of Fouks-Schubert transient correction method to
     point sources in ISOCAM data (September 1999)
Alain Coulais
TR: Characterization of memory effects affecting Fabry-Perot LWS
    line profiles  (September 1999)
Emmanuel Cau
TR: Transients correction tool based on the Fouks-Schubert method for
     SWS data available under OSIA (September 1999)
Fred Lahuis + Do Kester
SM: Definition of the RSRF for SWS; determination of the level
     of accuracy (September 1999).
Bart Vandenbussche
BP: New ISO Pointing reconstruction Cal-G files containing Tycho data
     for guide stars implemented in OLP (November 1999)
Andy Pollock
SM: Definition of a new RSRF for LWS  based on Uranus  observations
     (November 1999)
```

```
Tanya Lim
PH: Evaluation  of calibration improvements recently achieved
     and investigation on cross-calibration problems reported
     in the last Status  Report affecting OLP and/or  IA data
     with special emphasis on  OLPv8 data products  (November
     1998)

==============================================================================
        * Second Post-ops X-Cal. Status Report            01 Nov. 1999
             (on OLPv8)
==============================================================================
        * OLP 8.6 (LWS) IDC --> NDCs                      03 Nov. 1999
==============================================================================
        $ Delivery of Cal-G files for OLPv9.0             15 Nov. 1999
==============================================================================

GL: Characterization of glitch tails: final results (December 1999)
Ana Heras
PO: ISOPHOT Polarisation: final document (December 1999)
Ralf Siebenmorgen
LP: LWS line profile stability analysis: extension to a larger number of
     lines and targets, including: dependence on time and scan direction
     (January 2000)
Rosario Lorente

==============================================================================
        * Mid-term review                                 01 Feb. 2000
==============================================================================
        * OLP 9.0 (CAM) IDC --> NDCs                      03 Feb. 2000
==============================================================================
        $ Delivery of Cal-G files for OLPv9.2             11 Feb. 2000
==============================================================================

PH: Evaluation  of calibration improvements recently achieved
     and investigation on cross-calibration problems reported
     in the last Status  Report affecting OLP and/or  IA data
     with special emphasis on IA data products (April 2000)

==============================================================================
        * Third Post-ops X-Cal. Status Report             01 Apr. 2000
              (on IAs cross-calibration)
==============================================================================

SM: Analysis of spectral line fluxes; comparison between measurements on the
     same line obtained by different ISO instruments (April 2000).

GL: Implementation of a more sophisticated de-glitching method in PHT
```

```
     pipeline (May 2000)

=============================================================================
       * OLP 9.2 (PHT) IDC --> NDCs                       03 May  2000
=============================================================================
       * Deliveries for OLPv9.4 (SWS)                     15 May. 2000
=============================================================================

BP: Description  of  final  status  of  ISO Pointing reconstruction and
     improvements during post-operations (June 2000)
Andy Pollock + Alberto Salama
LP: LWS  line  profile stability analyisis:  dependence on detector and
     line strength and deviations from gaussian fit (June 2000)
Rosario Lorente
PO: ISOCAM Polarisation: final document (June 2000)
Ralf Siebenmorgen
GL: Implementation of improved  de-tailing algorithms in SWS IA (August
     2000).

=============================================================================
       * OLP 9.4 (SWS) IDC --> NDCs                       03 Aug. 2000
=============================================================================

GL: Implementation of glitch detection methods and de-glitching algorithms
     in CAM pipeline (August 2000)

=============================================================================
       * Deliveries for OLPv9.6 (major LWS upgrade)       15 Aug. 2000
=============================================================================

PH: Evaluation  of calibration improvements recently achieved
     and investigation on cross-calibration problems reported
     in the last Status  Report affecting OLP and/or  IA data
     with  special emphasis on  OLPv9  data products (October
     2000)

=============================================================================
       * Fourth Post-ops X-Cal. Status Report             01 Oct. 200
            (on OLPv9)
=============================================================================
       # Freeze calibration algorithms                    01 Oct. 2000
=============================================================================
       * OLP 9.6 (LWS) IDC --> NDCs                       03 Nov. 2000
=============================================================================
       $ Delivery of CAL_G for OLPv10                     15 Nov. 2000
=============================================================================
```

```
PO: Internal cross-calibration of ISO Polarisation measurements (December
     2000)

================================================================================
       * Official end of ISOSDC at MPE                    31 Dec. 2000
================================================================================

LP: LWS line profile stability analyisis: behaviour of point-like versus
     extended sources (January 2001)

================================================================================
       # Final reports on Calibration themes for post-ops 01 Feb. 2001
================================================================================
       * OLP 10.0 final OLP IDC --> NDCs                  05 Feb. 2001
================================================================================

PO: External  cross-calibration of ISO Polarisation measurements (March
     2001)

PH: Evaluation  of  calibration  improvements recently achieved
     and  investigation on cross-calibration  problems reported
     in the last  Status  Report affecting  OLP and/or  IA data
     with special emphasis on OLPv10 data products (April 2001)

================================================================================
       * Final Post-ops X-Cal. Status Report              01 Apr. 2001
           (on OLP v10)
================================================================================

LP: Comparison of results found both for LWS and SWS with the theoretical
     instrumental profiles and resolution (May 2001)
LP: Line profile definition, recommendations and caveats (May 2001)

================================================================================
       * ISO Explanatory Supplement final issue           01 May  2001
================================================================================
       * ISO PMA final delivery                           01 May  2001
================================================================================
       * End of ISO NDC at Saclay/Orsay                   31 Dec. 2001
================================================================================
       * End of ISO NDC at MPIA                           31 Dec. 2001
================================================================================
       * End of ISO NDC at RAL                            31 Dec. 2001
================================================================================
       * End of Post-operations Phase                     31 Dec. 2001
================================================================================
```

3 Internal and external cross-calibration

3.1 The concept of cross-calibration

- Cross-calibrations can be used (i) as consistency checks, and (ii) as true calibrations. In the first instance observations of a source by a pair of instruments are compared to evaluate internal consistency: if the results do not agree (to within the stated uncertainties) then the calibration procedure of one of the instruments (though possibly both) is incorrect. In the second instance, results from the less accurate instrument(s) are calibrated against data from the more accurate one(s).

In the case of ISO, the above concept can be applied both to pairs of ISO instruments that overlap in wavelength range and also to ISO instruments vs other non-ISO instruments.

3.2 Definition of standard and cross-calibration sources

- The absolute flux calibration of three of the four ISO instruments (CAM, PHT and SWS) is based primarily on results of the Ground-Based Preparatory Programme (GBPP, Jourdain de Muizon and Habing, 1992 Les Houches Series: Infrared Astronomy with ISO, p. 129) and of the Cohen, Walker, Witeborn et al. (CWW) absolute calibration programme (Cohen et al. 1992a AJ 104, 1650, 1992b AJ 104, 2030 and 1995 AJ 110, 275), though the long wavelength filters of PHT also use planets and asteroids to cover the bright and intermediate part of their dynamic range. The absolute flux calibration of LWS is currently based on Uranus as primary source.

- For cross-calibration purposes a small set of astronomical sources was used in the past. They include a few bright stars (like HR 7310, HR 7341, HR 6436, γ Dra or α Boo), planetary nebulae (NGC 7027 and NGC 6543), galaxies (Mrk 279), asteroids (Cybele, Hygiea) and planets (Neptune) on which most of the cross-calibration comparisons carried out so far have concentrated. For most of them observations exist taken throughout the whole ISO mission with more than one instrument and in many cases covering a wide range of wavelengths.

Note that, because of the limited common dynamic range between the ISO instruments, not all kind of inter-comparisons are possible. Stars are too faint in the long wavelength range of ISO to be used for cross-calibration analysis in the spectral region beyond 100 μm and asteroids and planets have to be used instead.

While the results of the CWW and the GBPP programmes, based on stars, are believed to be accurate to $\pm5\%$ or better and are consistent with one other, the uncertainties in asteroid and planet model spectral energy distributions are larger ($10-15\%$ level). In the case of asteroids their characterization is additionally complicated by their variability. Thus, the cross-calibration of LWS in the long wavelength range is especially difficult, since the comparison has to be made against PHT measurements, and the dynamic range overlap between PHT and LWS is limited.

Another important limitation is imposed by the fact that calibration problems do not necessarily affect all the cross-calibration sources in the same way. Thus, some comparisons do not shed any light on the understanding of a given problem if we restrict our analysis to the small sample of objects listed above.

3.3 Updated cross-calibration strategy

In order to take into account all the limitations and caveats considered above a modification of the cross-calibration strategy is needed. The following aspects need to be considered:

- First, cross-calibration must be able to ensure proper handling of differences in beam sizes, filter profiles and spectral resolution, as well as the use of differing absolute calibration systems and of different sets of astronomical standard sources.

- Second, the detailed investigation of specific calibration problems requires the selection of dedicated samples of targets - beyond the small list of astronomical sources listed above, used for general calibration purposes throughout the emission - containing a combination of bright/faint, red/blue, point/extended sources so that a complete picture of the impact of an existing problem on ISO data can be obtained or a new progress in data reduction can correctly be evaluated.

Of course, cross-calibration sources must have been observed with more than one instrument/configuration at least once during the ISO mission (for internal cross-calibration purposes) and/or infrared data from non-ISO instruments must be available (for external cross-calibration) and/or accurate models must exist against which ISO data can be compared (for absolute flux calibration).

- Last but not least, the adequate selection of a tool to be used for cross-calibration purposes during post-operations is also an important point to consider. The ideal cross-calibration tool should:

· be able to cope with a large number of data sets both of OLP and IA data products indistinctly in a fast and simple way.

· allow some basic manipulation (change of units, scaling, basic statistical analysis) of the data.

· provide the user with powerful (over-)plotting capabilities.

At the moment, several possibilities have been investigated:

- **IDA:** Unfortunately, the ISO Data Archive survey products display tools to be developed in the near future within the IDA environment do not consider the possibility of overplotting data corresponding to more than one observation, nor to carry out synthetic photometry on survey data products or any other similar functionality. This decision was taken by the IST in a previous meeting.

- **Atlas:** This is an IDL-based tool developed by Ekkehard Wieprecht and Alberto Salama which allows direct comparison of SWS and LWS ISO survey products. From an input list of TDT numbers created with an SQL query to the ISO Data Archive, it provides $m \times n$ plots on single pages for easy comparisons of a number of targets. Some IDL post-processing is also carried out by the Atlas tool like flux units conversion and automatic scaling for pairs of SWS-LWS spectra on the same target. It could be extended to PHT and CAM data with some manpower time and dedication. It can be very useful on a short time scale in its present form and until a new more powerful tool is available for the investigation of SWS/LWS cross-calibration aspects.

- **PIA:** Display tools currently exist under PIA that can easily be adapted to ingest and allow the overlapping of data corresponding to other instruments. This can be implemented with a small manpower effort. It would be desirable to have ready this possibility soon to deal with PHT, CAM and SWS cross-calibration comparisons before other tools are developed. Our recommendation is to encourage the implementation of these small changes in PIA so that on a short time scale cross calibration comparisons on PHT, CAM and SWS data could be carried out.

- **UDF:** Developed by E. Wieprecht and E. Wiezorrek, the User Defined Function (UDF) facility has recently been installed within the ISO Data Archive. This facility allows to query meta-information contained in a given observation. With a series of User Defined Functions it will be possible to extract virtual attributes from files external to the database engine. These virtual attributes can then further be used in queries inside the database engine. Eventually, when the necessary changes will be incorporated into the S/W, it will be possible to properly handle not only OLP data, but also data processed with any of the four instrument IAs. Thus, our final recommendation is, on a longer time scale, to encourage the use the UDF facility as the main tool for future cross-calibration comparisons.

3.4 Cross-calibration comparisons

One of the main goals of cross-calibration manpower at the IDC is to present, every six months in this series of Status Reports, the latest results derived from internal and external consistency checks that will be regularly carried out mainly by the Photometric Calibration WG. They will concentrate on OLP data products when a new OLP version becomes available and/or on IA data products when a new data reduction tool with expected impact on cross-calibrations is implemented.

In the following, some of the cross-calibration (internal and external) comparisons recently carried out are shown. The selection of results and analysis presented here put special emphasis on those cases where substantial progress has been achieved in the last few months or to illustrate a problem under investigation.

Note that, in the cross-calibration comparisons considered below, when they make use of pipeline data products, the analysis is based on files generated with OLPv7. When a problem/inconsistency was identified, further analysis was carried out using a more detailed data reduction with the corresponding IAs in order to try to understand the problem and determine whether it can be solved with the tools currenly available within the IAs or additional development is needed.

In future reports similar evaluations will be based on:

Issue	Date:	
#2	November 1999:	OLPv8 data products
#3	April 2000:	data processed with IAs
#4	October 2000:	OLPv9 data products
#5	April 2001:	OLPv10 data products (final report)

In most cases, overall agreement among the major instrument modes is found comparable to pre-launch expectations. In particular, at $\lambda \leq 50$ μm the results obtained exceed the expectations, especially for the spectroscopic modes, where agreement can easily reach the 10% level and better although, in some cases, this cannot be achieved at OLP level but requires some additional manual processing with IA, specially for CAM and PHT data. The situation is somewhat worse at longer wavelengths, as we will show below, where discrepancies are still sometimes larger than 20%, although this strongly depends on the brigthness of the source.

Application of adequate colour corrections to photometric filter measurements of very red/blue sources, beam profile corrections in the case of extended emission, removal of transient effects - which especially affect PHT and CAM data - and careful subtraction of dark current measurements for faint sources, among other possible corrections, usually improves the data accuracy significantly during post-processing using the corresponding IA software.

SWS versus model on Ceres

A comparison of SWS data with a termophysical model of the asteroid Ceres was carried out by Thomas Müller. The SWS observations are taken from a scientific programme by Alberto Salama and consist of a 2.3 h SWS06 scan with 1 up- and 1 down-scan per band. This leads to a full spectrum from 2.38 to 45.2 μm with a spectral resolution ranging from 1000 to 2000. Satellite tracking on Ceres was done with a 2 arcsec stepsize raster. The SWS06 data were

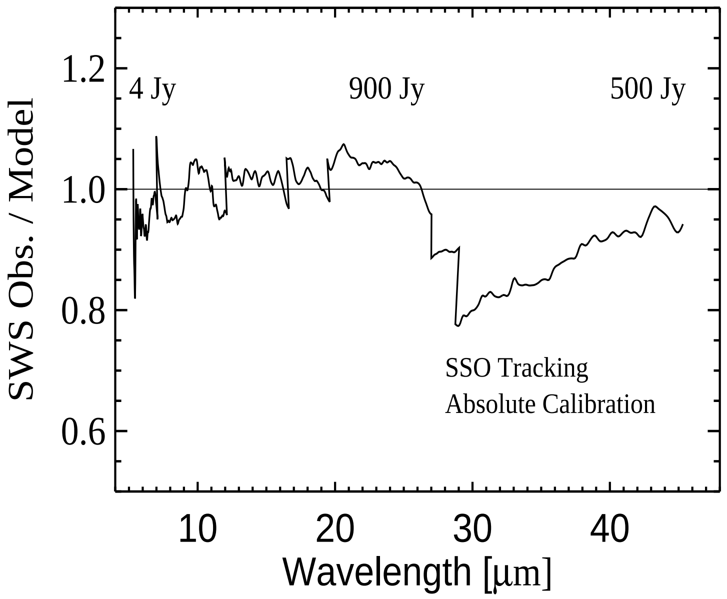

Figure 13: Ratio of ISO SWS06 observations to a termophysical model of Ceres. The numbers in the upper part of the diagram indicate the total flux level - Thomas Müller

processed with the standard product generation pipeline steps. After correction for the solar system tracking steps the final spectrum was obtained by sigma-clipping the data over bins with resolution 500 ($\sigma = 3$) and rebinning to the same resolution.

Figure 13 shows the ratio between the SWS observations and the model predictions. The thermal emission at wavelengths between 2 and 45 μm is within the 5 to 12% level of accuracy up to 27 μm and within 20-25% betwen 27 and 45 μm. The two steps at 26 and 29 μm are due to not perfectly corrected Solar System Object tracking. The different slope longward of 29 μm has also been observed in other objects with a similar spectrum, like Callisto, and is not yet fully understood. Even considering this problem, the results obtained match very well the expectations.

The complete report is available in *Fundamental thermal emission parameters of main-belt asteroids derived from ISO observations of Ceres* by Thomas Müller et al. (ISO Conference Proceedings, Paris 1998).

PHT-S and SWS versus model on Hygiea

A similar cross-calibration comparison was performed by Thomas Müller on the asteroid Hygiea this time using staring PHT-S observations and SWS data obtained at different epochs with ISO which were compared to a thermophysical model of the asteroid. The intention was to check the accuracy of SWS against the model and evaluate the improvement of accuracy provided by the new dynamic calibration method applied to PHT-S staring observations.

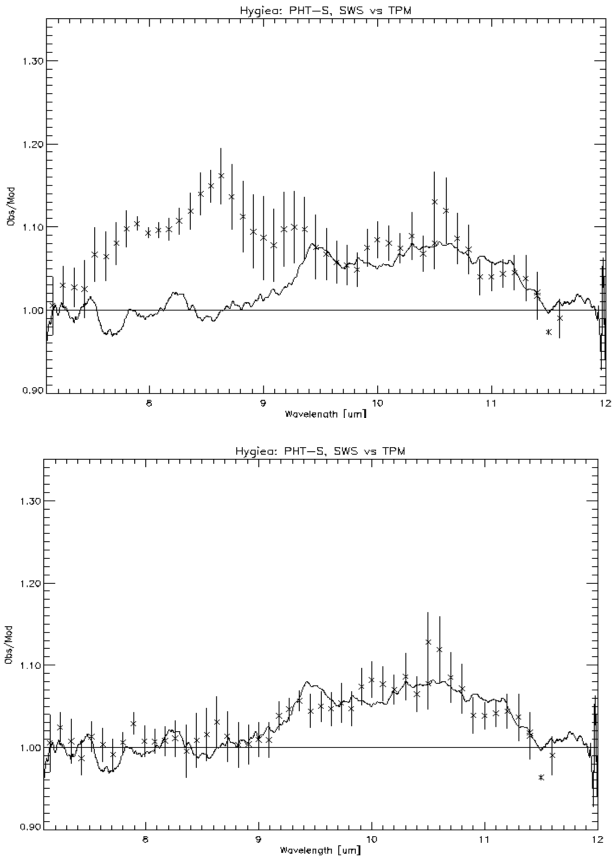

Figure 14: Ratio of ISO PHT-S and SWS observations to a termophysical model of Hygiea. The solid line is SWS while the crosses correspond to PHT-S data. In the upper panel we show the results obtained with the wrong standard star models; the lower panel shows the excellent results obtained when these stars are avoided - Thomas Müller

Figure 14 (upper panel) shows that the SWS measurement is in excellent agreement with the model (at the 3% level shortward of 9 μm and within 10% level in any case for the full spectral range). However, the dynamic calibration method applied to the PHT-S data produced at first a strong discrepant feature between 8 and 9 μm. After some investigation it was found that this feature was just an artifact, caused by SiO features not considered in the original models of the late type stars taken as standards and present in their spectra. Only excluding these stars from the generation of the calibration files (and hence accepting a large gap in the flux range covered by the calibration standards) the spurious features were eliminated in the calibrated spectra, as it is shown in the lower panel of Figure 14. Then the agreement between SWS and PHT-S is on the 3-4% level over the whole spectral range, while the excess of emission observed between 9 and 11.5 μm both in SWS and PHT-S with respect to the model seems to be a a real feature in the spectral energy distribution of Hygiea, not predicted by the model.

CAM filters versus chopped PHT-S on a sample of Seyfert galaxies

An excellent agreement can be obtained between chopped PHT-S measurements and CAM filter observations even for the case of very faint sources (a few mJy) although, in this case, a more sophisticated data reduction process is needed, since transient effects can be very important, especially in the case of the chopped PHT-S measurements.

As an example of this, we show here the results of a recent statistical analysis carried out on a sample of Seyfert galaxies observed with ISO. The observations are part of a scientific programme by Jean Clavel et al. and the full results are contained in an A&A paper submitted for publication.

In Figure 15 (courtesy of Bernhard Schulz) we can see two nice examples of PHT-S and CAM LW2 and LW7 filter measurements on the Seyfert galaxies Markarian 509 (Seyfert 1) and NGC 5953 (Seyfert 2). This Figure shows very clearly how Seyfert 1 galaxies are characterized by a strong continuum and faint PAH features, while Seyfert 2 are characterized by faint continuum and a strong PAH emission.

Seyfert galaxies in the sample were observed both with CAM LW2 and LW7 filters and with chopped PHT-S photometry. Manual recalibration of the spectra include glitch de-tailing and transient correction of the chopped PHT-S measurements. For the transient correction it is assumed that the initial response function of each pixel (we are only able to see the initial rapid jump of the transient in a short chopped measurement) can be calibrated against the behaviour of a standar star of similar brightness and observed under the same or very similar conditions (in this case, HD 132142). The results obtained are very satisfactory since the global median flux ratio (CAM filter/PHT-S) derived from the measurements is: 1.15 for the LW2 measurements and 0.94 for LW7, i.e. CAM flux densities without colour correction are only 15% higher in LW2 and 6% lower in LW7 than the corresponding PHT-S measurements.

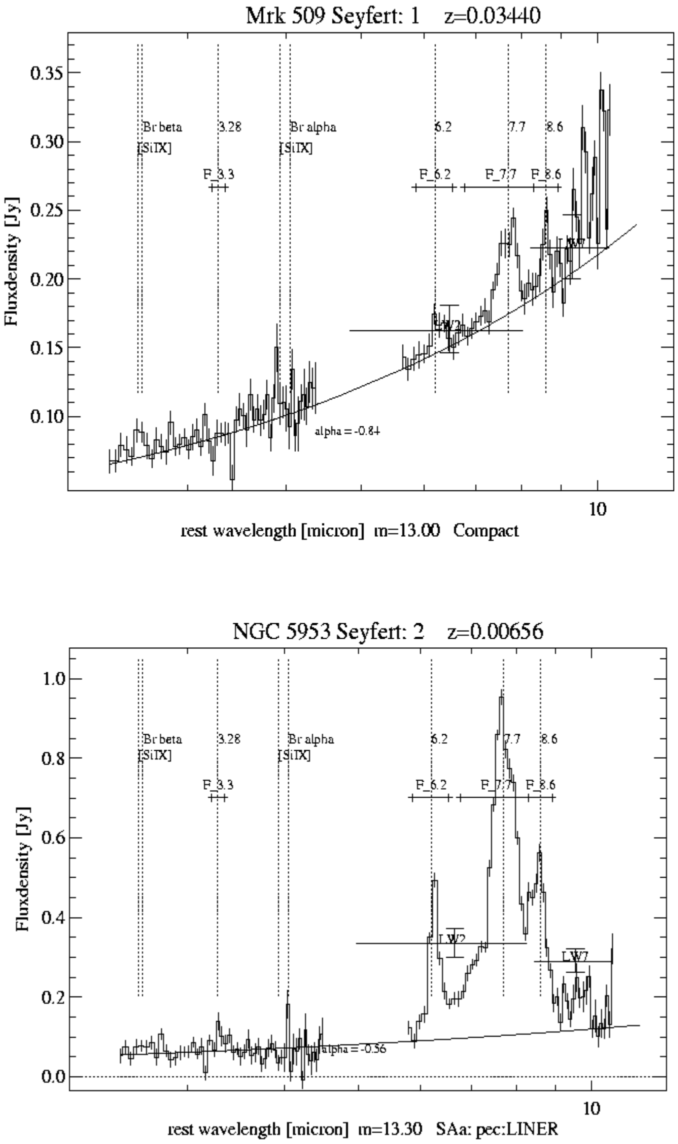

Figure 15: PHT-S spectrum and CAM LW2 and LW7 filter measurements for the Seyfert 1 galaxy Mrk 509 and the Seyfert 2 galaxy NGC 5953. The position of some of the more prominant lines is indicated - Bernhard Schulz

The colour correction for the large bandpass-filter could explain the difference for LW2 may be up to 10%, as the spectral energy distribution of the Seyfert galaxies observed are red, and with the PAHs contribution in the reddest part of the filter wavelength range. On the other hand, the higher fluxes detected in the LW2 5 - 8.5 μm filter might also be contaminated by the contribution from the stellar content of the underlying extended galaxy which may still be detectable even for the almost point-like Seyferts, CAM aperture being wider than the PHT-S one.

CAM-CVF and PHT-S versus model on Cybele

Joris Blommaert and Thomas Müller carried out a cross-calibration comparison of PHT-S and CAM-CVF observations on the asteroid Cybele. PHT-S and CAM-CVF data were obtained at different revolutions. Thus, the two spectra could not directly be compared as the flux of the asteroid is expected to change in time. For this reason the spectra were compared to model predictions provided by Thomas Müller. It turned out that the model predictions underestimate the fluxes for both CAM-CVF and PHT-S data. In both cases, the initial model had to be multiplied by 1.45 since it was found that the absolute flux of Cybele was also deviant in comparison with other calibrators for other PHT-measurements (the model will be further investigated).

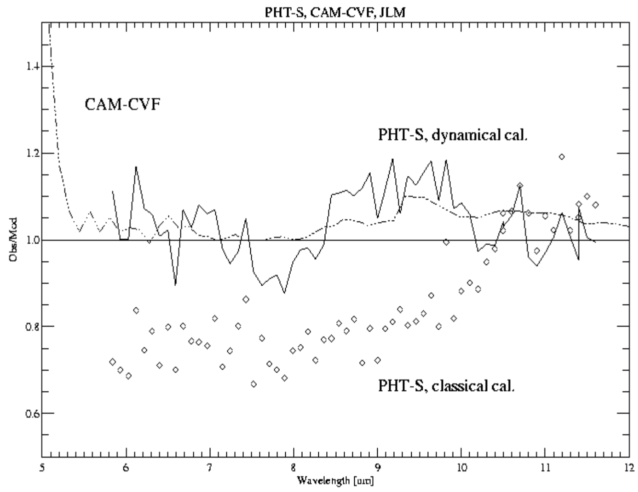

Figure 16: Ratio of ISO CAM-CVF and PHT-S observations to a termophysical model of Cybele. The dashed line corresponds to CAM-CVF. PHT-S data is shown before (diamonds) and after application of the new dynamic calibration (solid line) - Joris Blommaert

With respect to the shape of the spectrum, the PHT-S spectrum was calibrated in two ways (by Thomas Mueller). First, using the old RSRF and second, using the new dynamic calibration method.

Figure 16 shows the PHT-S dynamic-calibrated spectrum together with the PHT-S spectrum calibrated using the old RSRF. The latter shows a slope that differs from what is predicted by the model and leads to deviations of up to 20% with respect to the CAM-CVF data. The comparison of the CAM-CVF spectrum with the dynamic-calibrated PHT-S spectrum is very good instead, and deviations are smaller than 5%. Both spectra agree very well with the corrected model spectrum.

The discrepant CAM-CVF values observed at the shortest wavelengths is explained by a strong transient effect, which is evident in the individual up- and down-scans taken not correctly removed. Note that Cybele is very faint at short wavelengths ($\sim$0.1 Jy at 5 μm) and that, for simplicity, a simple average of the two spectra was used to roughly correct for the transient effects in the CVF spectrum, which worked well for most of the spectral range observed, but not for the very blue edge where a more detailed transient correction is needed.

SWS/LWS comparison at 44 μm

Using the Atlas tool, a cross-calibration comparison of a flux limited ($>$ 100 Jy at 44 μm) sample of targets from the ISO Data Archive observed both with SWS01 and LWS01 was carried out by Alberto Salama.

122 different astronomical sources were selected and investigated in order to evaluate the degree of matching between SWS and LWS observations in the overlapping region. Some of them were observed several times during the mission. The consistency found between independent measurements taken on the same source with the same instrument is within the 10% level for LWS and the 20% level for SWS.

After sigma-clipping ($\sigma = 2$) and rebinning, the median value of the spectral region between 43.7 and 44.4 μm was derived for both SWS and LWS. This median was used to derive the LWS/SWS ratios at 44μm, which are found to range from 1 to 6 with about 50% of them within $\pm$20% from unity (see Figure 17).

Values larger than unity would be expected from the ratio of beam sizes if extended sources are among the sources selected in the sample. Note that the FWHM of the LWS beam at 44μm (SW1 detector) is 71" while the aperture of SWS band 4 at this wavelength is a rectangular box 20" $\times$ 33" in size which gives a beam ratio LWS/SWS of $\sim$6.1.

Variability should also be investigated in order to explain the mismatching cases.

They are currently being investigated by Pedro García-Lario in detail in order to determine whether a calibration problem exists (see list of new actions above). A first look at the individual data indicates that most of the SWS and LWS observations were taken simultaneously. Thus, variability should not play

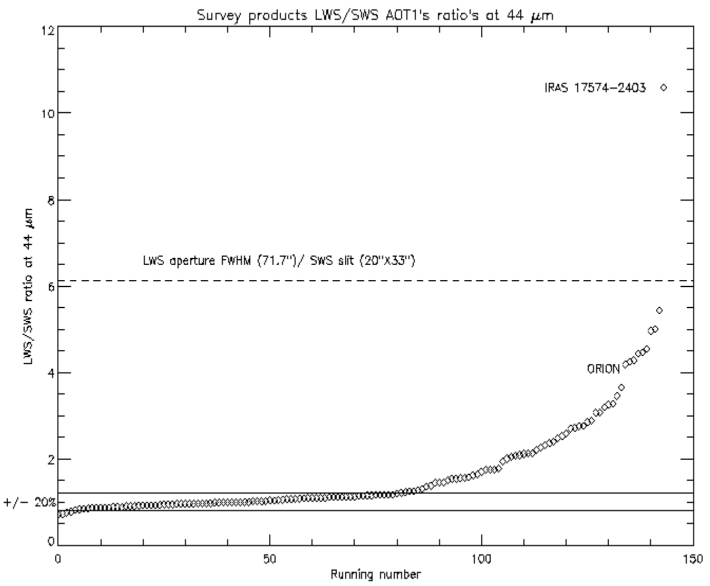

Figure 17: Distribution of LWS/SWS ratios observed at 44 μm - Alberto Salama

any role in the mismatches observed and can be discarded.

Instead, a correlation is found between the discrepant cases found at 44μm and jumps observed at 27.5 and 29.0 μm in the same sources. These wavelengths coincide with changes in the apertures from band 3D to 3E at 27.5μ (the aperture increases from 14" $\times$ 27" to 20" $\times$ 27") and from band 3E to 4 at 29.0μm (the aperture increases from 20" $\times$ 27" to 20" $\times$ 33"). This seems to confirm the initial guess of the extended nature of the sources observed being the main reason for the large LWS/SW ratios observed.

Pierre Cox is also making a comparative study on selected compact HII regions with similar preliminary results. Further investigation is also still ongoing.

PHT-C filters, LWS filters and LWS scan versus model on Ceres

A number of LWS02 fixed grating position measurements at 8 different wavelengths, namely 46.1, 56.2, 66.1, 75.7, 84.8, 102.5, 122.2 and 141.8 μm, one full LWS scan and several PHT-C200 filter measurements (at 120, 150, 170, 180 and 200 μm) taken at many different epochs have been analized and compared with a termophysical model of the asteroid Ceres.

The data processing of the LWS observations started with the AAR OLP products on which manual deglitching was performed. Several LWS detectors showed a slow rise of signal during the observations in the photometric mode. In

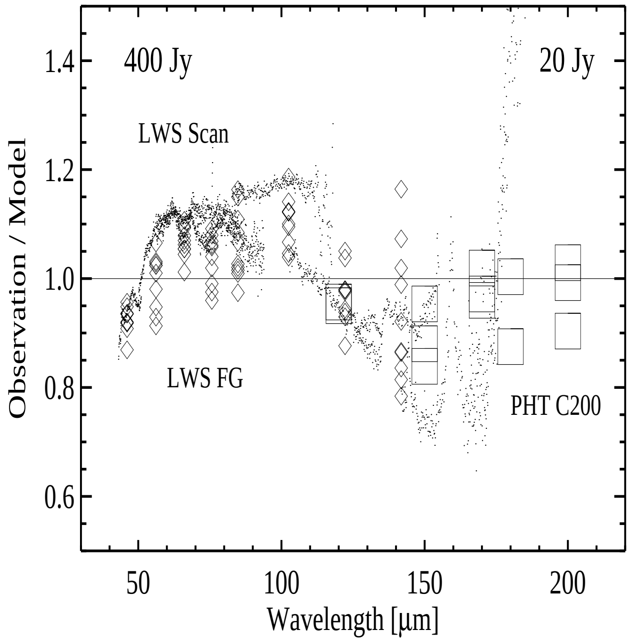

Figure 18: Ratio of ISO LWS and PHT-C observations to a termophysical model of Ceres. Diamonds represent the LWS fixed grating (FG) observations, the squares are the PHT-C observations and the dots belong to the full LWS scan.

these cases only the the last part of the integration time was used to determine the flux. Technical problems affected the long wavelength part (LW2 to LW4) of the LWS scan.

The PHT data were taken at 4 different epochs with the C200 camera using the special Calibration Uplink System (CUS) mode of observation. Each observation consists of 2 internal reference measurements (FCS) and a 4×4 raster on source with the source centered in each pixel for 2-4 min. The data have been partly processed with PIA v7.1 and partly manually outside PIA. The standard data reduction included linear ramp fitting, deglitching on ramp and signal level, reset interval correction and orbit dependent dark current subtraction. The calibration is based on the comparison with standard stars measured in exactly the same observing mode, which makes the calibration possible for each of the 4 detector pixels individually and independently. With off-source observations taken into account, an absolute accuracy of 5 to 10% is reached.

Figure 18 shows the ratio of the ISO observations to a termophysical model of Ceres. The general agreement is in the order of 10% between the LW filters, the LWS scan and the PHT-C measurements, although there is a large scatter, especially at the longer wavelengths. The increase in the LWS scan beyond 170 μm is caused by a technical problem during the observations.

The stronger discrepancy observed when the ISO data is compared to the model might be due to the fact that the emissivity model is not correct and that there is a decrease in emissivity beyond 100 μm larger than the one predicted by the model.

The complete report is available in *Fundamental thermal emission parameters of main-belt asteroids derived from ISO observations of Ceres* by Müller et al. (ISO Conference Proceedings, Paris 1998)

ISO data versus non-ISO data

Here we report on the external cross-calibration comparison carried out by Thomas Müller on a sample of 10 asteroids used as far-IR calibrators for ISOPHOT.

The ISO data were compared via asteroid models to ground-based mid-infrared and sub-millimetre/millimetre observations, IRTF (infra Red Telescope Facility), JCMT (James Clerk Maxwell Telescope), HHT (Heinrich Hertz Telescope), and IRAS (Infrared Astronomical satellite) data. For this, the various inband fluxes were converted to individual monochromatic flux densities. This way, a total number of 678 individual observations ranging from 7 to 2000 μm were compiled.

The ISOPHOT measurements consist of PHT-C calibration measurements carried out with ISO (asteroids are considered as photometric standards in the intermediate range of brightness beyond 50μm) on the 10 asteroids listed in Table 1. In this case, the asteroids were calibrated determining the FCS at high flux levels using only measurements on planets and at low flux levels using only stars. The asteroid measurements can then be treated as independent specific observations. The bright ones can be compared against the planets Uranus and Neptune, whereas the faint ones are close to the flux densities of the brightest standard stars.

The observing mode of centring the source on each detector pixel provides in case of C100 (9 pixels) and C200 (4 pixels) several independent measurements of the same object within a few minutes. The observing sequence is accompanied by background and dark current measurements, leading to reliable asteroid fluxes with an uncertainty of 10%. In total, 35 individual photometric data points were derived between 50 and 200 μm.

The 10 asteroids observed were divided into two groups of so-called primary and secondary calibrators depending on the coverage and quality of the data available. The asteroids Ceres, Pallas, Vesta and Herculina were selected to be primaries, and the remaining ones to be secondaries, although there are still clear differences in quality within these groups.

With the assumed thermophysical models of each of the asteroids in the sample a cros-calibration comparison was carried out in order to check their

Table 1: Expected uncertainties derived for each of the 10 asteroids used as far-IR calibrators by ISOPHOT as a function of the wavelenght range (from 7 to 2000 μm)

Asteroid	7−13	13−24	24−500	500−1200	1200−2000
1 Ceres	0.059	0.091	0.098	0.045	0.126
2 Pallas	0.077	0.061	0.087	0.057	0.166
4 Vesta	0.048	0.076	0.088	0.108	0.104
532 Herculina	0.106	0.101	0.111	0.136	0.329
3 Juno	0.089	0.185	0.086	-	-
10 Hygiea	0.172	0.287	0.117	0.107	-
54 Alexandra	0.119	-	0.137	-	-
65 Cybele	0.209	0.049	0.187	-	-
106 Dione	0.307	-/321	0.285	0.235	-
313 Chaldaea	0.085	0.152	0.139	0.207	-

reliability. For each data point in the database the ratio of predictions and observations were compared. The r.m.s. of the mean values found are displayed in Table 1 grouped by wavelength bins and represent the expected uncertainties when using the asteroids for photometric calibration at different wavelengths.

In the case of ISOPHOT data the r.m.s associated to the primary standards is about 10% and usually below 15% (with the exception of Dione and Cybele) for the secondary standards.

The complete report is contained in *Asteroids as far-infrared photometric standards* by Müller & Lagerros (A& A 1998, 338, 340)

4 Calibration accuracies and 'Error Budget'

The currently expected uncertainties affecting the calibration accuracy of ISO data are reported in a series of documents which are regularly issued and updated by the different instrument teams. They are used as a reference for cross-calibration purposes. Apart from that, the expected uncertainties introduced in the calibration of ISO data at each relevant processing step per observation mode, the so-called Photometry 'Error Budget', are also described in dedicated documents on a per instrument basis.

- **SWS:**

  - The latest report available on the instrument accuracy of SWS is contained in *SWS Calibration Status*, available at:

  `http://www.iso.vilspa.esa.es/users/expl_lib/SWS/SWS_Cal_Accuracy.html`

  which describes the updated status of absolute flux calibration of SWS data as of March 1999 and from which a large fraction of the information below has been extracted.

  For SWS the goals originally set before the mission (an accuracy of 30% or better) have, in general, been achieved for well-behaved data sets. By well-behaved data sets we understand point sources in the several hundred to several thousand Jansky flux density range that were observed with correct pointing and suffered no instrumental or operational problems.

  In Table 2 an overview of flux calibration accuracies of SWS OLP products is given as a function of the SWS band considered. The quoted 'worst' uncertainties are primarily valid for the edges of the bands, representing the maximum product of the absolute and relative spectral responsivity uncertainties. The accuracies given here were determined in June 1997 for version 6 of the pipeline.

  The flux reproducibility was checked during the mission by regular observations of the calibration star HR6705. The various measurements agreed to within 6% for band 1 and 2 to 15% for bands 2 to 4.

  Unfortunately, an 'error-recipe' for the combination of all the known individual error contributions to a useful overall error estimate for SWS data products does not exist yet.

  The problem is that the relevance of the various error contributions depends strongly on the properties of the observed source as well as on the type of scientific analysis that is aimed for.

  Thus, no 'error budget' in the true sense can be given, but it is possible to provide the user with an indication of the currently known error contributors.

Table 2: Overview of the SWS bands and flux calibration accuracy

	Band	Key wavel. μm	Grating order	Aperture number / area "	Detector type	Detector pixels	Wavelength range μm	Accuracy key - worst
SW	1A	2.48	SW4	1 / 14x20	InSb	1 - 12	2.38 - 2.60	5% - 7%
	1B	2.87	SW3	1 / 14x20	InSb	1 - 12	2.60 - 3.02	5% - 7%
	1D	3.08	SW3	2 / 14x20	InSb	1 - 12	3.02 - 3.52	5% - 7%
	1E	3.80	SW2	2 / 14x20	InSb	1 - 12	3.52 - 4.08	5% - 7%
	2A	4.50	SW2	2 / 14x20	Si:Ga	1 - 12	4.08 - 5.30	7% - 12%
	2B	5.90	SW1	2 / 14x20	Si:Ga	1 - 12	5.30 - 7.0	7% - 15%
	2C	7.70	SW1	3 / 14x20	Si:Ga	1 - 12	7.0 - 12.0	11% - 25%
LW	3A	14.0	LW2	1 / 14x27	Si:Ga	1 - 12	12.0 - 16.5	11% - 25%
	3C	17.0	LW2	2 / 14x27	Si:Ga	1 - 12	16.5 - 19.5	11% - 20%
	3D	24.0	LW1	2 / 14x27	Si:Ga	1 - 12	19.5 - 27.5	12% - 20%
	3E	28.5	LW1	3 / 20x27	Si:Ga	1 - 12	27.5 - 29.0	20% - 30%
	4	32.0	LW1	3 / 20x33	Ge:Be	1 - 12	29.0 - 45.2	30% - 35%
	5A	11.8	LW3	1 / 10x39	Si:Sb	1 - 2	11.4 - 12.2	11% - 25%
	5B	14.8	LW2	1 / 10x39	Si:Sb	1 - 2	12.2 - 16.0	11% - 20%
	5C	17.0	LW2	2 / 10x39	Si:Sb	1 - 2	16.0 - 19.0	11% - 20%
	5D	24.0	LW1	2 / 10x39	Si:Sb	1 - 2	19.0 - 26.0	12% - 30%
	6	27.0	LW1	3 / 17x40	Ge:Be	1 - 2	26.0 - 44.5	30% - 35%

Generally, for well-behaved data sets, the use of OSIA's tools does not lead to significant improvement in the calibration with the exception of data affected by the presence of interference fringes in band 3 and, to a lesser degree, in band 2.

For data sets that are not well-behaved the quoted accuracies are not reached with standard OLP processing. However, often manual processing using OSIA tools allow to reach the same level of accuracy.

Some of the known sources of error are:

Detector memory effects: Band 2 (Si:Ga) and band 4 (Ge:Be) are especially affected. Currently, a correction for these effects is not yet available although a transient correction based on the Fouks-Schubert model applicable to band 2 data will probably be implemented in OSIA soon. The signature of memory effects is that the up- and down-scans are different in flux level. The down-scan normally succeeds the up-scan in the AOT and appears to be already 'accustomed' to the flux level. Thus, one procedure that has been used to improved data affected by memory effects is to take the down-scan as the reference for the flux level.

Dark current problems: dark currents corrupted by memory effects or glitches usually result also in systematic differences between the up- and down-scans. For large errors in the subtracted dark current, the final spectra will resemble the spectral responsivity. Unfortunately, small dark current problems and memory effects have a similar signature in the final spectra.

Fringes: Bands 2 and 3 can be affected. The amplitude and frequency of the fringes depend on the source morphology, brightness and position in the SWS entrance aperture. Fringe amplitudes of about 5% of the continuum level are seen in band 2 and up to 20% in band 3. Fourier filtering or sine fitting can be used to remove the fringes 'manually'.

Pointing Offsets: As a consequence of the non-uniformity of the detector material and small internal misalignments, the signals in the different AOT bands are reduced by band-dependent factors when a point source is observed with a pointing offset with respect to the centre of the SWS aperture. Corrections for this effect can only be applied when the detailed beam profiles have been determined and the actual satellite pointing is known with sufficient accuracy. Pointing offsets are recognized by jumps in the continuum level at band edges in AOTs 1 and 6. In AOT 2 data the effect is very difficult to see.

Glitches: All SWS detector data suffer from cosmic ray hits. Some of them are removed automatically, but especially in the long wavelength bands the removal is far from complete. Tails following a cosmic ray hit are usual in these bands. Currently, they can only be removed manually within OSIA.

Extended sources: SWS calibration is based on point source emission. As a result, the fluxes derived are not appropriate for extended sources (partially) filling the SWS aperture. At the band edges, jumps in the signal level are seen, which are due to changes in the effective size of the detectors. To obtain reliable flux densities for extended sources, the SWS detector beam profiles should be convolved with the source structure at the appropriate wavelength. As a first order correction, the ratio of the aperture sizes can be taken.

Very weak sources: For very weak sources careful inspection of the data is required to be able to filter out data affected by glitches and determine the true dark current level, while fringes are normally insignificant. Proper calibration and analysis of such data is only possible with much manual labour.

Very bright sources: Very bright sources suffer mainly from memory effects and fringes. The data may also be affected by detector saturation which starts to become important at the several 10000 Jy level. Again, manual labour is needed to deal with such observations.

Some improvements are hoped to be achieved during the post mission phase with respect to the calibration accuracy of SWS. They include improvements in the determination of the Relative Spectral Response Function and the characterisation of detector memory effects and of the beam profile.

A better understanding of the memory effects will lead to higher accuracies in band 2 and band 4 flux calibration scale (see recent achievements in the *Transients WG* section). In the area of extended sources, calibration improvements are expected also very soon once the characterization of the SWS beam profile is completed (see *Beam Profiles WG* section). It is, however, not obvious how to automatically apply such corrections because this requires the introduction of information about the source structure into the OLP environment which is *a priori* unknown.

An additional important goal for the OLP processing is to make the errors as given in the SWS data products (SPD and AAR) a useful quantity. With respect to this, an agreement has been reached so that from OLPv8 onwards, uncertainties in flux calibration of data products will be specified and made up from three parts: standard deviation (from the fitting of the ramps themselves), offset (from dark current correction) and gain.

- **LWS:**

  - The latest report available on the accuracy of LWS, as of November 1998, is contained in: *LWS Calibration Status*, available at:

  `http://www.iso.vilspa.esa.es/users/expl_lib/LWS/LWS_Cal_Accuracy.html`

  This report is based on OLPv7 data products. Most of the comments below are based on the information contained in this document. A summary of the main results is displayed in Table 3 as a function of the AOT and the brightness of the source. Note that the concept of 'bright', 'medium' and 'fain' source depends on the observing mode. For the grating modes a 'bright' source means typically more than 1000 Jy at 120μm, while 'faint' could be a source with a flux density in the order of 10$-$50 Jy at 120μm. For the fabry-Pérot modes these numbers have to be multiplied by a factor of 10 at least.

  Fabry-Pérot AOTs are not yet validated owing to a problem of misalignment of the underlying grating response profile. This is caused by uncertainty in the grating wavelength calibration.

  Some of the known sources of error affecting LWS are:

  Relative Spectral Response Function: detailed examination of the shape of the continuum of Mars and other Solar System objects indicates that the Uranus model used as primary standard shows a discrepancy at the shortest wavelengths (43 $-$ 55 μm) at the level of no more than 7% at the extremes of the SW1 band and this is being investigated.

Table 3: Flux calibration accuracy of LWS OLPv7 data products per AOT

		LWS01 Grating	LWS02 Grating	LWS03 Fabry-Pérot	LWS04 Fabry-Pérot
Point sources	Bright	30%	30%	Unvalidated	Unvalidated
	Medium	10%	10%	Unvalidated	Unvalidated
	Faint	50%	50%	Unvalidated	Unvalidated
Extended sources	Bright	50%	50%	Unvalidated	Unvalidated
	Medium	30%	30%	Unvalidated	Unvalidated
	Faint	50%	50%	Unvalidated	Unvalidated

Dark current subtraction and memory effects: this especially affects spectra of faint sources. There is evidence that observation of a bright source before a faint one has caused the dark current to be higher than expected and to be decaying during the subsequent observation. In addition, dark current variations have been observed within Fabry-Pérot measurements which are presently not fully understood.

Fringes: channel fringing is seen on the measured spectra of extended or off-axis point sources. Extensive modelling of the response of the instrument has been carried out using the ASAP optical design software showing that the fringes are produced by the interference between the reflecting surface of the LWS field mirror and its support structure as the diffraction pattern of the source falls off the edge of the field mirror itself. A quantitative model, however, is not yet available that would allow the removal of the fringes given knowledge of the spatial structure of the source. Instead, a method has been developed which performs a fit for the period, amplitude and phase of the sinusoid and removes it from the spectrum by division or subtraction.

Beam profile: the pipeline processing of LWS data makes no attempt to correct for the beam shape of the instrument. Attempts have been made to determine the spatial response of LWS using spectra of Mars located at different positions with respect to the axis of the LWS as a function of wavelength. The FWHM of the esentially gaussian beam profiles obtained are ~20% narrower than expected. In addition, the beam is assymetric and fringes are also present. Detailed analysis is on-going (see *Beam Profile WG* section).

Non-linearity effects: Bright sources cause some of the detectors to become non-linear. The problem is complicated by photon curing of the detectors; this, in turn, causes the responsitivity of the detectors to change. An empirical method has been developed and implemented in the pipeline for the derivation of the photocurrent, and hence flux, from the voltage

Table 4: Flux calibration accuracy of LWS LIA data products per AOT

		LWS01 Grating	LWS02 Grating	LWS03 Fabry-Pérot	LWS04 Fabry-Pérot
Point sources	Bright	30%	30%	50%	50%
	Medium	10%	10%	30%	30%
	Faint	50%	50%	50%	50%
Extended sources	Bright	50%	50%	50%	50%
	Medium	30%	30%	30%	30%
	Faint	50%	50%	50%	50%

ramps which fits a first or second order polynomial automatically with no *a priori* assumptions about how the detectors respond, reducing the noise in the output spectra.

Time constants: The time constants of the detectors cause the shape of the spectrum (both lines and continuum) to be distorted under certain illumination conditions.

Poor order sorting: Spectra below 50 μm and between 83 and 90 μm might suffer from contamination owing to poor order sorting. An instrument model is required that will allow the determination and removal of the contamination.

The calibration accuracy of products manually processed with LIA does not significantly improve for the grating observing modes LWS01 and LWS02 for well-behaved data sets. The only changes expected concern LWS03 and LWS04 as can be seen in Table 4 below. For bright sources observed with these AOTs there is an excess component in the signal that is most likely due to straylight.

A discussion on the individual contribution to the LWS photometry 'error budget' coming from the different steps involved in LWS data processing is contained in the document: *In-orbit performance of the ISO Long Wavelength Spectrometer* by Bruce Swinyard et al. (October 1998), available at:

`http://www.iso.vilspa.esa.es/users/expl_lib/LWS/HAWAII.PS`

Assuming a mean uncertainty in the Uranus model of ~5% and a statistical error on the RSRF better than 0.01, for observations where the dark current is not a significant contribution to the signal, the uncertainty contributed to the measurement by the calibration process is estimated to be of the order of 7% for most detectors. In the case of faint sources, when the dark current becomes significant, the uncertainty in the measurement of the dark current begins to dominate.

Long term monitoring has shown that the repeatability of the flux calibration is within 10% for all objects not influenced by the uncertainty in the dark current measurement.

For LWS the goals originally set before the mission (an accuracy of 30% or better in the grating mode and 50% in the Fabry-Pérot mode) have in most cases been achieved for well-behaved data sets. In some areas, however, problems remain and they are the subject of further investigation.

The flux calibration accuracy of LWS is expected to improve during the post-operational phase.

- The discrepancy in the shape of the Uranus spectrum is expected to be fully characterized soon. If and when confirmed, an improvement of the continuum determination at short wavelengths should be expected.

- Interpolated beam maps, as a function of wavelength for each detector should also be available on a short time scale. The absolute accuracy that will be achievable in these maps is difficult to estimate at present but the aim is to have an accuracy not worse than 10% at 1% of the beam profile. Estimating the systematic error on the flux calibration of a source of arbitrary distribution within the beam at any wavelength is problematic as it is likely to be a function of wavelength due to the more precise sampling of fringes at longer wavelengths.

- The characterization of the behaviour of the detector dark current following observations of bright sources is also expected to improve. This may lead to an improvement in the systematic error in the flux determination for some faint sources.

- Detailed studies of the response of the detectors to strong sources are on going and more sophisticated methods of dealing with the problem are being investigated. It is to be expected that this problem will be solved for the final archive.

- The temporal response of the detectors is another problem to be dealt with for point sources. To date no real effort has been put into the problem. The problem has to be addressed and, again, we will aim for a systematic error of no more than 10% for any point in the spectrum.

- **PHT:**

  The latest report on PHT calibration accuracy is contained in the document *ISOPHOT Calibration Accuracies* by Ulrich Klaas et al. (October 1998) available at:

  `http://www.iso.vilspa.esa.es/manuals/PHT/accuracies/pht_accuracies20/`

Most of the information presented here is based on this document.

In Table 5 we give an overview of the wavelength range covered by the different subinstruments and detectors of PHT together with the typical aperture sizes.

Table 5: Covered wavelength range and typical aperture sizes of ISOPHOT subinstruments. Note that for PHT–C the first aperture number denotes the pixel size, the second one the array size.

subinstrument	**detector**	**dimension**	**wavelength range** [μm]	**typical aperture size** [“]
PHT–P	P1	1	3 – 17	5 – 180
	P2	1	15 – 29	23 – 180
	P3	1	40 – 130	52 – 180
PHT–C	C100	3x3	40 – 130	43.5 / 138
	C200	2x2	100 – 240	89.4 / 182
PHT–S	SS	1x64	2.5 – 4.8	24
	SL	1x64	5.8 – 11.8	24

Absolute and relative accuracies as well as relative flux reproducibility are based on the analysis of OLPv7 data products. Note, however, that a number of AOTs are not yet scientifically validated (see Table 6) and, thus, no global accuracies can be provided. In addition, the two polarisation modes PHT50 (PHT-P) and PHT51 (PHT-C) are processed by the pipeline only to raw data level and are not here considered. It is the goal of ISO Post Operations to scientifically validate the OLP processing of all standard AOTs in Table 6 for which this is pending. A rough schedule of improvements which will be implemented in upcoming versions of the pipeline is given in this Table.

Table 7 gives a summary overview of the currently achieved photometric accuracies with PHT and the reproducibility of the observations.

The use of OLP data products for the estimation of the calibration accuracy allows a homogeneous comparison of data sets and the estimation of commonly applicable uncertainties. However, careful interactive analysis using PIA can sometimes significantly improve the calibration accuracy of PHT data. Unfortunately, it is not possible here to give numbers as a function of the AOT and/or the characteristics of the source observed since so far no comprehensive systematic investigation was performed. But one can expect to achieve a higher accuracy using PIA in the following cases:

Table 6: Status of scientific validation of PHT OLP AOT processing as of version 7.

AOT	**observation type**	**submode**	**scientifically valid since**	**next upgrades**	**foreseen in OLP Vx.y**
PHT03 (P)	multi-	staring point source	V6	non-lin R & FCS aper	8.4
	filter	staring ext. source	no	beam	8.4
	photometry	nodding	V6	non-lin R & FCS aper	8.4
		chopped point source	no	chop	8.4
		raster map	no	map cal & drift	8.4/9.2
PHT04 (P)	multi-	staring point source	no	beam & FCS aper	8.4
	aperture	staring ext. source	no	beam	8.4
	photometry	chopped point source	no	chop & beam	8.4
PHT05 (P)	absolute	staring point source	V6	FCS aper	8.4
	photometry	staring ext. source	no	beam	8.4
PHT17 (P)	sparse map	staring point source	V6	non-lin R & FCS aper	8.4
18 , 19	photometry	staring ext. source	no	beam	8.4
PHT22 (C)	multi-	staring point source	V7	non-lin R	8.4
	filter	staring ext. source	V7	non-lin R	8.4
	photometry	nodding	V7	non-lin R	8.4
		chopped point source	no	chop	8.4
		raster map	no	map cal & flat-field	9.2
PHT25 (C)	absolute	staring point source	V7		
	photometry	staring ext. source	V7		
PHT32 (C)	oversampled	chopped mapping	no	chop & map cal	9.2
	mapping				
PHT37 (C)	sparse map	staring point source	V7	non-lin R	8.4
38 , 39	photometry	staring ext. source	V7	non-lin R	8.4
PHT40 (S)	spectroscopy	staring point source	V5		
		staring ext. source	V6	beam	8.4
		chopped point source	V6		
PHT50 (P)	aperture	staring point &	V7	interactive processing	
	polarimetry	ext. source		& special FORTRAN routine	
PHT51 (C)	array	staring point &	V7	interactive processing	
	polarimetry	ext. source		& special FORTRAN routine	
		raster	V7		

meaning of calibration upgrades:

non-lin R	: correction for non-linearity of detector responsivity for data sets covering a wide flux range
FCS aper	: correction for inhomogeneous illumination of PHT-P apertures by FCS
beam	: beam profile corrections
chop	: chopped photometry corrections
map cal	: surface brightness calibration in maps
drift	: correction of non-linear long-term drifts
flat-field	: refined flat-field corrections

Table 7: ISOPHOT Photometric Calibration Accuracy Overview.

detector	**source type** point / extended	**source brightness**	**typical on-source integration** [s]	**absolute accuracy** [%]	**reproducibility** $1\,\sigma$ **of 20 samples** [%]	**multi-filter accuracy** [%]
P1	p	50 – 6000 Jy	32	10	5	20
P1	p	0.1 – 50 Jy	$\leq$ 256	30	10	TBD
P2	p	10 – 200 Jy	32	$<$ 15	2	10
P2	p	0.5 – 10 Jy	$\leq$ 256	$<$ 20	12	TBD
P3	p	0.5 – 25 Jy	32	15	7	20
P3	p	$<$ 0.5 Jy	$\leq$ 256	30	7	TBD
C100	p	0.5 – 25 Jy	32	10	$\geq$ 3	10
C100	p	$<$ 0.5 Jy	$\leq$ 360	30	20	TBD
C100	e	5 – 15 $\mathrm{MJy\,sr^{-1}}$	32	20	10	$<$ 30
C200	p	1 – 900 Jy	128	20	10	TBD
C200	p	0.2 – 1 Jy	$\leq$ 240	30	10	TBD
C200	e	4 – 10 $\mathrm{MJy\,sr^{-1}}$	64	20	6	$<$ 30
SS	p	2 – 5000 Jy	256	$<$ 30	$<$ 30	$<$ 30
SS	e	50 – 10^5 $\mathrm{MJy\,sr^{-1}}$	256	$<$ 30	$<$ 30	$<$ 30
SL	p	1 – 5000 Jy	256	$<$ 30	$<$ 30	$<$ 30
SL	e	50 – 10^5 $\mathrm{MJy\,sr^{-1}}$	256	$<$ 30	$<$ 30	$<$ 30

1) measurements with signal transients which do not stabilise during the measurement time, but which are long enough to perform a reasonable transient fit.
2) flat-fielding of maps, depending on the sampling mode and the dynamic range.
3) correction of non-linear signal drifts in maps.
4) detection of faint sources by refined deglitching and filtering.

The impact of each calibration step on the accuracy of the PHT OLP version 7.0 of the pipeline up to the SPD level is described in detail in *ISOPHOT Error Budget: Derive_SPD Processing Steps* by Rene Laureijs and Ulrich Klaas (April 1999), available at:

`http://www.iso.vilspa.esa.es/manuals/PHT/error_budget/error_budget05/`

In a later version of this document the 'error budget' up to the AAR level will also be included.

The different calibration steps are described in detail in this document with their limitations and applicability. In addition, the uncertainty/noise introduced in the process of data reduction is discussed in terms of systematic uncertainties, photometric bias, relative accuracies, detection limits and flux reproducibility.

It includes the analysis of the effects produced by:

- discarding non-linear and saturated read-outs,
- ramp linearization in PHT-P and PHT-C,
- ramp deglitching,
- extraction of signal from first order polynomial fits,
- selection of a given reset interval length in PHT-P, and PHT-C
- dark signal subtraction,
- signal deglitching,
- discarding signals in chopped measurements,
- transient recognition,
- signal averaging per chopper plateau,
- chopper vignetting/offset correction in PHT-C,
- determination of in-band power from FCS,
- determination of detector responsivity in PHT-P and PHT-C,
- determination of the default detector responsivity,
- aperture scaling of FCS measurements in PHT-P,
- correction for inhomogeneous FCS illumination in PHT-C,
- detector pixel filter-to-filter response correction in PHT-C,

In addition, a summary of the photometric uncertainties introduced by background subtraction as a function of the photometric method used is also given. This correction is especially important in the observation of faint sources, for which the simpler observing modes (off-on) are much less accurate than the ones optimized for faint source observation (telescope nodding for PHT-P and mini-maps for PHT-C).

Some other instrumental effects, however, are not considered since there are not yet corrections available for them in OLPv7.0. This is the case of responsitivity transients and responsivity non-linearities. Corrections for these two important sources of error are available under PIA (see comments on this under the *Transients WG* and *Photometric Calibration WG* section of this document, respectively).

P1 and PHT-S detectors cause the largest responsivity transients with the effect of a photometric bias of more than 100% for large flux steps and short (32 s) integration times. Typical observations that can be affected at a level higher than 20% of accuracy are:

- observations with detectors P1, P2 and PHT-S.
- multi-filter observations with PHT-S and relatively short integration times ($t_{int} \leq 64$ s); faint targets are more affected because the relaxation time is generally longer.
- PHT32 maps with high dynamic range. For very high dynamic range maps 'ghosts' of bright point sources have been seen about 1 chopper sweep away from the actual targets.

Concerning responsivity non-linearities, the problem consists on the use of an FCS measurement which is not at an adequate power level. Typical observations affected by non-linearity are:

- multi-aperture photometry of extended sources when moving from a small aperture to a large one can easily give a factor of 10 increase in power on the detector. Note that the FCS is always tuned according to the brightest flux.
- multi-filter photometry using filters with large differences in transmission or on targets with a steep spectrum (like stars).
- maps with a high dynamic range. Usually the FCS is tuned according to the flux of the brightest source in the map; therefore, the photometry of the weaker sources in the map will be biased and/or the morphology of bright extended sources will be distorted.

A number of goals have been defined for the improvement of PHT absolute and relative multi-filter photometry to be achieved by the end of ISO Post Operations.

These are, for point sources:

- absolute accuracy in bright sources: 10% ($f_{\nu} > 2$ Jy on intermediate background brightness, minimum on-source exposure time: 32 s)
- absolute accuracy in faint sources: 20% ($f_{\nu} < 2$ Jy on, S/N > 10, minimum on-source exposure time: 128 s)
- relative filter-to-filter accuracy: 10%
- absolute accuracy in PHT-S: < 20%
- relative accuracy in PHT-S: < 20%
- absolute accuracy in chopped modes: <30%
- flux reproducibility for both bright and faint sources: <10%

For extended sources:

- absolute accuracy: <20%
- relative filter-to-filter accuracy: <20%
- for PHT-P the same quality as for PHT-C, independent of aperture size.

On a short time scale the main calibration upgrades expected for OLPv8.4 are those incorporated in Table 6 and include:

- correction for non-linearity of detector responsivity for data sets covering a wide flux range in PHT-P and PHT-C measurements
- correction for inhomogeneous illumination of PHT-P apertures by the FCS in PHT-P measurements
- new beam profile corrections
- new chopped photometry corrections in multi-filter/aperture PHT-P and PHT-C photometry of point sources

- **CAM:**

The latest report on CAM accuracy is provided in the *ISOCAM Calibration Acccuracies Document* by Joris Blommaert and Diego Cesarsky (November 1998) available at:

`http://www.iso.vilspa.esa.es/manuals/CAM/accuracies/cam_accur/`

An overview of the flux accuracy of the different CAM OLP data products is given in Table 8 for two different brightness levels. The numbers in this Table are based on the analysis of standard stars observed in the central part of the array and on OLP version 7.0 data products. Note that although polarisation observations (CAM05) are handled by the current version of the pipeline, the corresponding observing mode has not formally been released yet.

A description of the known sources of error affecting CAM calibration and the corresponding 'error budget' is contained in *The ISOCAM Calibration Error Budget Report* by Andrea Biviano (November 1998), available at:

Table 8: ISOCAM Photometric Calibration Accuracy Overview.

CAM AOT	> 100 mJy	<100 mJy
CAM01	20%	30%
CAM03	20%	30%
CAM04	40%	40%
CAM05	-	-

http://www.iso.vilspa.esa.es/users/expl_lib/CAM/errdoc.ps.gz

The following sources of error are identified:

- **Glitches:** the contribution of glitches to the overall noise of CAM images is important. 'Common' glitches are associated to impacts of cosmic ray electrons while the so-called 'faders' and 'dippers' are linked to impact of protons or α particles. Tipically, 'common' glitches are easy to remove while the rare 'faders', followed by a slow decrease of the signal, and 'dippers', followed by a reduction in the sensitivity of the affected pixel, have a long lasting effect more difficult to remove. Unfortunately, since the detection of glitches in the pipeline is based on simple median filtering algorithms, only a fraction of them are automatically removed and manual processing with CIA is needed.
- **Transients:** in general, the dominant error source in CAM images are transients, for which no correction is implemented in the pipeline. Thus, the use of CIA routines is also needed if we want to improve the accuracy of CAM data affected by transients. In particular, most of the CVF observations are usually performed after a discrete filter observation, thus implying a large decrease in the incident flux on the detector. This can introduce important transient effects that last several readouts and hence several wavelength steps. The result is a larger than true flux for the first wavelength steps. We also know that transients are more important for weak sources than for bright sources and this is the most important reason for the differences in the uncertainties quoted in Table 8.
- **Point Spread Function:** the fluxes for point sources in the CPSL (CAM Point Source List) FITS file are derived by PSF-fitting in the image. This photometry can be affected by larger errors than stated in Table 8 if the fitting is incorrect. The observed PSF is generally quite close to the theoretical one if the ghost contribution is not significant (see below). However, the accuracy of the PSF does not allow deconvolution yet.
- **Flat-field:** because of wheel-jitter the 'library' flat-field may not cover the same detector region as the sky image does. The effect is small in the central region of the array where the uncertainty is less than 1%. The uncertainty becomes, however, very large in the edges (up to a factor of 5 in extreme cases), where vignetting is important (for example in the case of a 6" PFOV measurement). Incomplete stabilization is another issue to consider. A large part of the small residual error in the flat-field observations is probably due to this effect. In any case, the noise levels reached are lower than expected pre-launch (1% in LW and 3% in SW).

- **Ghosts:** CVF observations might be affected by the existence of 'ghosts' generated by multiple reflections between the detector and the CVF surface. Ghosts can appear away from the source image but may as well fall onto (and surround) the sky image, depending on the actual position of the source on the detector. In some cases, the photometric accuracy can be affected up to 25% by the presence of ghosts, and straylight from sources outside the theoretical field of view can affect CVF images so that sources with a flux below 10% of the background are not detectable.

Other error contributors like saturation, read-out, gain accuracy, dark current stability are also discussed in the 'error budget' document above refered. A summary of the main conclusions is displayed in Table 9.

Table 9: ISOCAM photometric calibration error budget.

Noise origin	magnitude	after correction
Stabilization (random)	10 x sky noise	2 x sky noise
Stabilization (systematic)	40% of source flux	15% of source flux
Saturation	$\geq$30% decrease in responsivity	
Read-out noise	LW: 0.7 ADU/g	
	SW: 2 ADU/g	
Gain	0.15% output current	
Dark current	LW: 0.5 ADU/g	0.25 ADU/g
	SW: 0.5 ADU/g	
Flat-field	LW: 0.5% (high background)	
	SW: $\leq$ 1%	
Conversion signal$\rightarrow$flux	5%	
Point Spread Function	20%	few%
CVF RSF	3%	
Ghosts	$\leq$30%	
Straylight	10% of sky flux	

Regarding flux reproducibility, repeated photometric observations on HIC 89474 throughout the whole ISO lifetime give a standard deviation of around 2% for both LW and SW detectors. Similar observations on a larger set of absolute flux calibration standards give an r.m.s. of around 5%. It was also found that the LW detector is very linear over a very large range of flux levels from a few mJy up to the saturation level. From CVF observations the derived r.m.s. is 3% for the SW part and 4% for the two LW CVF segments.

Significant improvements in the photometric accuracy of ISOCAM data can be achieved by making use of the software tools implemented in CIA, the Interactive Analysis software package for ISOCAM data reduction.

Deglitching routines are available under CIA although they only mask the frames corresponding to the glitches. Thus, a visual inspection of all pixels histories is needed for a proper masking. The impact of 'faders' and 'dippers' is related to the general problem of the transient behaviour of the CAM detectors and can be corrected using transient correction algorithms implemented in CIA, based on the so-called 'IAS method' (for LW detectors).

In general, the systematic errors introduced by incomplete stabilization can be reduced up to a 10-15% level with the IAS method and can be better than 1-2% after the application of the new transient correction routines based on the Fouks-Schubert's model in the case of CVF spectra affected by large transients inherited from previous discrete filter observations. However, the method still fails for structures with strong spatial gradients (like point sources).

Manual elimination of ghost images, which can in some cases lead to errors up to 25% in aperture photometry, is also possible with CIA, as well as the elimination of inaccuracies introduced by inaccurate flat-fields, at least in the case of rasters with sufficient background and redundancy (not possible, however, for staring observations yet).

In summary, the magnitude of all the above effects compared to pre-launch expectations are generally in good agreement. Note that in Table 9 the 5% accuracy quoted as error induced by the conversion factor from ADU/g/s to Jy is worse than the pre-launch value (2%) because the measured photometry is PSF corrected, so this error estimate includes also the uncertainty in the PSF.

The CVF Spectral Response Function (SRF) is very well constrained. Typically the accuracy is at the 3% level on average in the absence of ghosts and straylight.

Concerning the expected accuracies of ISOCAM's final OLP data products, this will strongly depend on whether the calibration improvements that are now available under CIA can be transfered into the OLP pipeline (we know that, certainly at least for transients, the problem of implementing the corresponding corrections in the pipeline is far from simple).

5 Conclusions

Most of the results presented above are quite satisfactory. In particular, the spectroscopic modes compare reasonably well, exceeding pre-launch expectations. In general, overall calibrations have improved significantly in the last few months and they are expected to significantly improve also in the near future.

The new dynamic calibration method applied to PHT-S staring measurements, already available in PIA, which has now reduced the previously observed discrepancies with CAM-CVF data below the 5% level, and the new Fouks-Schubert's transient correction method, recently implemented in CIA, which allows to reach accuracies below the 3% level when applied to CAM observations of extended sources, represent just two examples of the strong progress achieved in the last few months.

Very soon other calibration improvements will be implemented either in the OLP pipeline (version 8) or in the instrument IAs. They have already been refered to along the document and their effects on the improved calibration accuracy of ISO data will be analized in subsequent issues of this Cross-calibration Status Report with the help of the updated cross-calibration strategy described in this document.

Among the expected improvements we can cite:

- the new correction for non-linearity effects on PHT data and the new method to correct multi-filter/aperture PHT measurements for transient effects, both available in the next version of the pipeline,

- the improved calibration of extended objects and not well-centred objects observed with SWS and LWS that will be possible when the beam profile models will be available,

- the determination of new more accurate RSRFs both for SWS and LWS,

- the characterization of the detector memory effects observed in some SWS bands,

- the application of the Fouks-Schubert's transient correction method to point sources observed with CAM or

- the understanding and characterization of ghosts and straylight affecting also CAM data.

Probably, the weakest point of cross-calibrations as they are understood at the present stage, and one of the conclusions that can be extracted from this report, is the fact that, in many cases, the acquired knowledge on a given calibration aspect and/or the major data reduction improvements achieved so far have only been implemented into the instrument IAs and not into the pipeline. In some cases, with only some additional effort, the implementation will be possible in the future and this should be encouraged. However, sometimes because the algorithms to be implemented need of some interactive manipulation, sometimes because they make use of 'a priori' assumptions, like the spatial structure of the source, the improvement will never be transferable to an automatic pipeline.

This is very much related with the reliability of the ISO Data Archive as a tool for external users and the exploitation of the ISO Legacy which must be a common worry shared by the IDC and the NDCs and will probably deserve additional thinking.